LBL-26557

Lawrence Berkeley Laboratory
UNIVERSITY OF CALIFORNIA

EARTH SCIENCES DIVISION

Contaminant Plume Monitoring Adjacent to the Kesterson Reservoir, California

N.E. Goldstein, S.L. Pillsbury, J.S. Daggett,
and S.M. Benson

June 1989

Prepared for the U.S. Department of Energy under Contract Number DE-AC03-76SF00098.

DISCLAIMER

LBL-26557

Contaminant Plume Monitoring Adjacent to the Kesterson Reservoir, California

Norman E. Goldstein, Stacey L. Pillsbury, John S. Daggett, and Sally M. Benson

Earth Sciences Division
Lawrence Berkeley Laboratory
1 Cyclotron Road
Berkeley, California 94720

June 1989

This work was supported by the U.S. Bureau of Reclamation, under U.S. Department of Interior Interagency Agreement 8-AA-20-06330, through U.S. Department of Energy Contract DE-AC03-76SF00098.

Abstract

Detailed ground conductivity surveys have been made twice with the Geonics EM31 and EM34 systems over a 2 km^2 area adjacent to Ponds 1, 2 and 5 of the Kesterson Reservoir. In spite of relatively high and variable near-surface conductivities, the first survey in October 1987 indicated that the saline agricultural groundwater discharge into Kesterson Reservoir between 1981 and 1986 had migrated a maximum lateral distance of about 300 m from Pond 2, the most intensively used storage pond. To determine the extent to which the contaminant plume was changing as a consequence of pond flooding with less saline, native groundwater starting in 1986, we conducted a second survey in October 1988, almost exactly one year after the first survey. Reanalysis of the 1987 data was done in conjunction with analysis of the 1988 data. Comparisons of the two data sets indicate that the shallowest soils and sediments, those within the first 2 to 3 meters of the surface, are less conductive in 1988. As supported by water level data in a number of observation wells along the edge of the survey area, and further confirmed by numerical modeling, the lower ground conductivities near the surface are due to a deeper water table and a reduction in average water saturation in the unsaturated zone. The cessation of pond flooding in 1987, possibly coupled with low 1987 rainfall, was primarily responsible for the less conductive near-surface conditions. To delineate the extent of a plume of saline groundwater in the saturated zone, the apparent conductivity data derived from the EM31 and EM34 measurements were plotted as isoconductivity contours and as variable dot-density pixels. In particular, after transforming the data to emphasize conductivities in the saturated zone, it is very apparent that areas of conductive groundwater exist adjacent to all three ponds; the largest anomaly is adjacent to Pond 2 which was the principal inlet point for the saline agricultural drainage water. To define the position of the plume better and to obtain quantitative estimates for conductivities in the saturated zone, 1-D numerical inverse modeling was done along a profile over the anomaly adjacent to Pond 2. These calculations suggest that the conductivity of the groundwater immediately adjacent to the reservoir, hence pore water salinity, has decreased slightly between 1987 and 1988. This change is consistent with diminu-

tion of the saline plume due to mixing with the less saline groundwater used to flood the reservoir from 1986 to 1987. However, we are unable to discern advancement of the leading edge of the saline plume away from the ponds. This is due to the relatively large survey line spacing of 100 m, which limits resolution, and the low velocity of groundwater flow.

Introduction

A detailed ground conductivity survey was made in October 1987 over private land (the Fremont Ranch) adjacent to Ponds 1, 2 and 5 of the Kesterson Reservoir, Merced County, California (Fig. 1). Conductivity anomalies two to three times greater than background values were found adjacent to the ponds (Goldstein et al., 1988). This finding confirmed an earlier hydrologic study which indicated that saline drainwater (conductivity 1000 to 1700 mS/m) used to flood the ponds between 1981 and 1986 had penetrated a near-surface layer of clayey soils and sediments and had infiltrated a sandy aquifer. There the drainwater would have mixed with the native groundwater (conductivity in the range of 300 to 400 mS/m), and then migrated subradially away from the reservoir. To determine the extent to which the saline plume was migrating as a consequence of flooding the ponds with less saline, native groundwater starting in 1986, we conducted a second survey in early October 1988, one year after the first survey. The same type equipment and survey techniques were used, and the original stations were reoccupied.

In this report, we discuss the results of the ground conductivity resurvey and attempt to quantify and analyze the differences between the 1987 and 1988 measurements in terms of changes in groundwater conditions.

Background

Between 1981 and 1986 the U.S. Bureau of Reclamation discharged agricultural drainwater via the San Luis Drain into the Kesterson Reservoir (Fig. 1). Most of the water entered Pond 2; occasionally Ponds 1 and 12 were inlets to the reservoir. Water entering Pond 2 flowed both northward and southward into other ponds. Consistent with this pattern of pond filling, the most extensive subsurface migration of the saline plume appears to be associated with Pond 2 (ESD, 1987).

Although selenium in the drainwater was found to be retarded by chemical reactions in the chemically reducing pond-bottom sediments, the non-reactive components of the saline

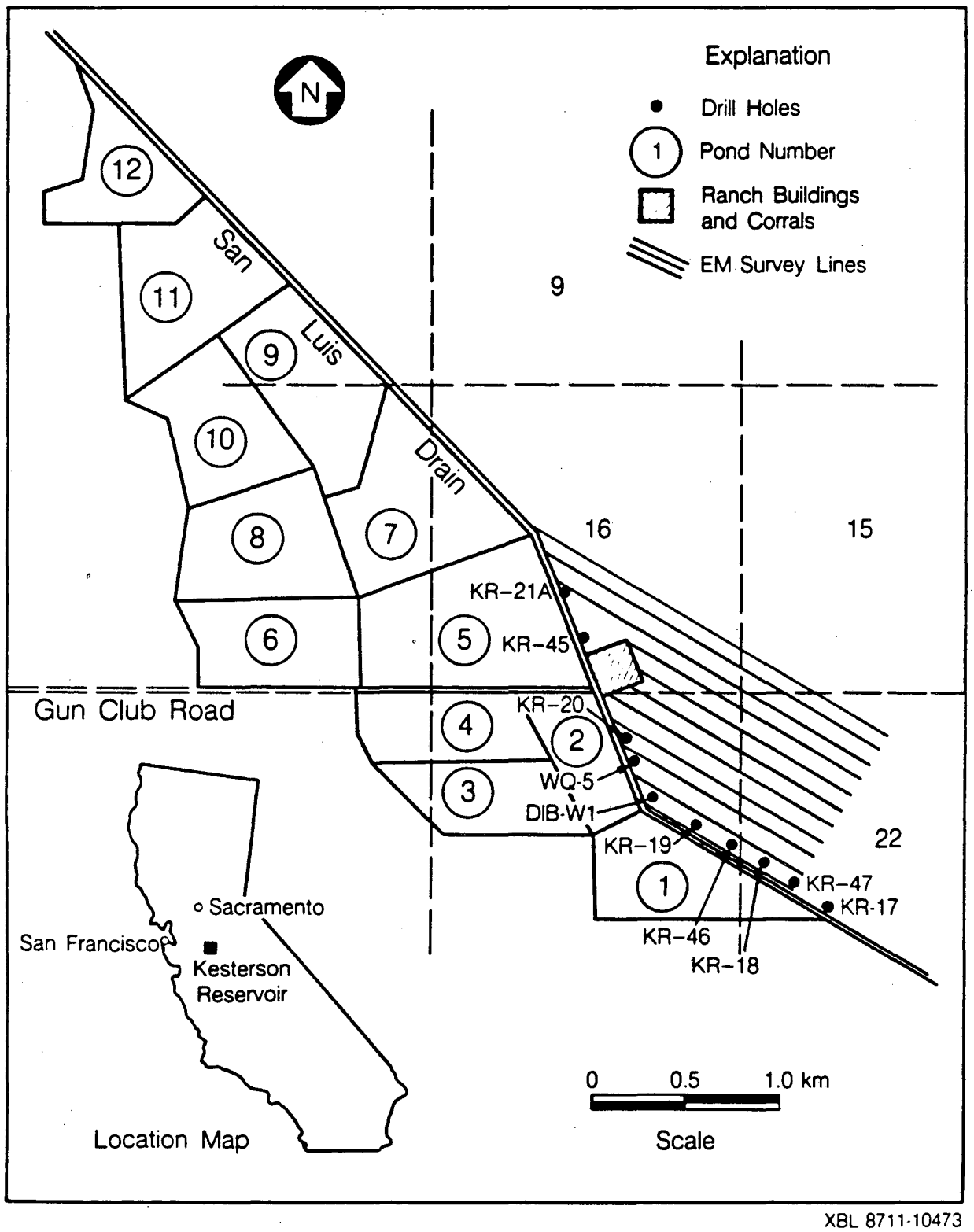

Figure 1. Location map of the Kesterson Reservoir showing the ponds, ground conductivity survey lines, and observation wells.

waters had infiltrated a shallow sandy aquifer beneath the ponds and were suspected to be migrating eastward down the regional hydraulic gradient toward Salt Slough. To quantify the possible migration of the saline plume, a two-dimensional radially symmetric flow model was devised to simulate migration of a non-reactive chemical plume (ESD, 1986). For the four-year simulation, corresponding to years 1981-1985, the chemical front migrates to a depth of about 20 m below the surface, and to a lateral distance of approximately 160 m from the edge of the reservoir (Fig. 2). These calculations did not consider hydrodynamic dispersion. Consequently, the leading edge of the plume is expected to be underestimated by these calculations. Nevertheless, they provide guidelines for assessing potential migration of the saline groundwater.

An opportunity to confirm these numerical results was obtained in October 1987 when the first of two ground conductivity surveys was conducted over the Fremont Ranch property adjacent to and east of Ponds 1, 2 and 5 (Fig. 1). Measurements were made using the Geonics EM31 and EM34-3 ground conductivity meters, two commercially available electromagnetic instruments whose depths of investigation depend on coil geometry and ground conductivity. Under the highly conductive ground conditions at the Fremont Ranch the depth of investigation is limited to depths of approximately 10 m below the surface (see Appendix A). The results of those measurements showed areas of increased ground conductivity adjacent to all three ponds with the largest anomaly adjacent to Pond 2 where the leading edge of the conductor appeared to extend a distance of approximately 300 m from the San Luis Drain (Goldstein et al., 1988). The leading edge of the conductor was not well resolved for two principal reasons: the coarse survey line separation and the inherent limitations of electromagnetic techniques to resolve the dispersed leading edge of a conductive plume.

In 1986, the practice of flooding the ponds with saline agricultural drainwater was discontinued. From then until December 1987, less saline native groundwaters were added in varying amounts to Ponds 1, 2, 5, and 7 in order to maintain anoxic conditions in the pond bottom sediments. It was also anticipated that flooding the ponds with less saline water would have two

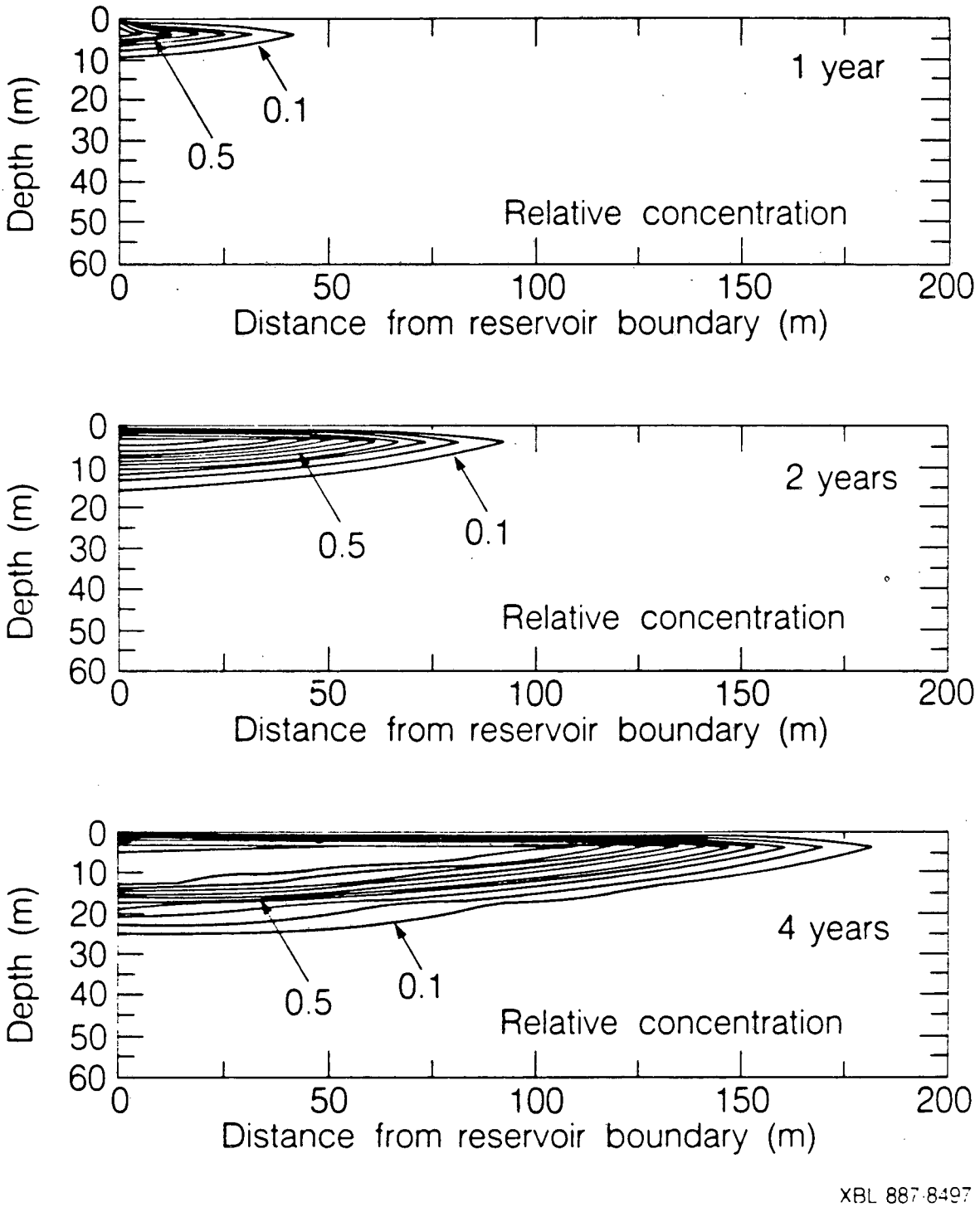

Figure 2. Simulated predictions for the migration of a conservative chemical species moving subradially away from the flooded Kesterson Reservoir. Contours are concentrations relative to the concentration of the species in the reservoir. Year 0 corresponds to 1981, year 4 to 1985.

effects on groundwater quality. First, the hydraulic influence of the flooded ponds would cause the saline plume to continue to migrate at a rate similar to past rates. Second, the salinity of the water under and immediately down-gradient of the reservoir was expected to decrease due to infiltration of less saline waters. To determine the extent to which these processes were occurring, a repeat ground conductivity survey was carried out in early October 1988, almost exactly one year after the original survey. By repeating the survey at the same time of the year we hoped to minimize seasonal effects, such as rainfall, evaporative flux, and water table depth, which affect ground conductivity readings. So that the results could be compared, the 1987 survey was duplicated as closely as possible; the same instrument types (but not the same units) were used, and the same measurement procedures were followed. Also, a transit survey was carried out to re-establish the original lines. One factor we could not control was the drier, hence less conductive, soil conditions due to cessation of flooding Kesterson Reservoir and reduced seasonal rainfall during the 1987-1988 period.

The Survey Site

Ground conductivity measurements were made over a portion of the Fremont Ranch, just east of the San Luis Drain and adjacent to Ponds 1, 2 and 5 of the Kesterson Reservoir. The survey area is located in Section 15, 16, 21 and 22, T.8 S., R. 10 E., 13 miles north of Los Banos and 7 miles east of Gustine in the San Joaquin Valley (Fig. 1). The area is covered by the U.S. Geological Survey San Luis Ranch and Ingomar 7.5-minute quadrangle topographic sheets.

The average elevation of the area is 21.5 m above mean sea level. The surface topography varies from flat near the drain to slightly undulating to the east in the direction of the several natural drainage features. The principal natural feature is an intermittent stream channel or slough which cuts across the southeast part of the area. The channel, dry during the survey, carries seasonal runoff in a northerly direction into Salt Slough. A saline depression, presumed to be a relict feature of the ancestral San Joaquin River system, exists at the south

end of the survey area. Salt crystals, desiccation cracks, and a field check in March 1989 show that this depression, dry at the time of the survey, is seasonally flooded by rising groundwater and/or rainwater. The entire survey area is criss-crossed by meter-wide man-made canals that once distributed waters to the area. The ranch is used for cattle and horse grazing.

The survey was conducted during the first two weeks of October 1988. Days were dry and warm (70-80°F); nights were cool. Traces of rain fell twice during the second week of the survey and wetted the first few millimeters of ground. However, calculations discussed in this report show that a very thin conductive surface layer would have negligible effect on the conductivity meter readings.

Geology

Knowledge of the near-surface geology of the survey area is largely based on detailed examinations of a suite of cores taken to depths of 6 to 10 m at points within Ponds 1 and 2 and a suite of geophysical logs from 18 wells in the vicinity of the reservoir. Two generalized lithologic units have been identified in the top 20 m below the ground surface (Flexser, 1988; ESD, 1987). The upper unit, 2 to 4 m thick, contains clay-rich and poorly sorted sediments varying from clay to clayey sand and silt. These sediments were deposited in a marsh environment probably not unlike the present-day marshes around Kesterson. Calcite, varying from sparse disseminated grains to thick concentrations and nodules, occurs throughout the upper unit, indicative of soil development, both modern and ancient, under arid to semi-arid conditions.

Measurements made on core samples of the near-surface soils taken from test plots in Ponds 8 and 9 (July 1988 - Jan. 1989) show that evaporative fluxes increase salt concentration in the soil during the summer months. The mass ratio of total water-soluble salts, e.g., $Na_2 SO_4$ and NaCl, to soil peaks at 80 to 90 mg/gram in the October-November period (ESD, 1989). In spite of the highly saline conditions, the resulting loss of soil porosity and lower saturation may make the upper 0.1 m more resistive during these months. With the onset of the rainy season in November-December, infiltrating rainwater tends to dissolve and redistribute the

more soluble salts, thus increasing near-surface conductivity.

The clay-rich upper unit grades into a lower unit composed mainly of well-sorted but unconsolidated sands and gravels derived from granitic rocks of the Sierra Nevada and deposited as channel and overbank sediments by the San Joaquin River and its associated sloughs. Coarse arkosic sand and gravel become abundant with depth, indicating deposition by broad, braided streams. Thin intervals of finer sediments, silts and clays, also occur within the lower unit and show evidence of soil development.

Flexser (1988) studied selected samples of the cores by microscopic analysis (of the sand size fraction) and x-ray diffraction (of the clay size fractions). Sands of both the upper and lower units are mineralogically similar, composed mainly of quartz and feldspar derived from Sierran granite. The lower unit also contains minor lithic fragments of andesite and schist from the Sierra foothills, and rare clasts of chert and graywacke from Coast Range rocks.

There is substantial uniformity, as well, in the clay mineral compositions. Figure 3 is a clay and silt depth profile taken at LBL site 4 in Pond 1 (ESD, 1986a). Here the upper unit is mainly a sandy loam, containing an average of about 15% clay fraction. The peak at 2.75 m depth corresponds to a thick unit classified as a silty clay loam. In both units smectite and kaolinite are the dominant clay minerals. The relative clay concentrations are as follows:

Smectite > Kaolinite >> Chlorite > Illite.

Because smectite has a high cation exchange capacity, rocks and soils with this mineral may have a bulk conductivity in excess of that predicted by ionic conduction in the pore fluids alone (Waxman and Smits, 1968; Bussain, 1983; Clavier et al., 1984). Here, however, the bulk conductivity of the soils is dominated by ionic conduction due to the very saline pore fluids. Consequently, the effect of variable clay content was not considered in this analysis of the ground conductivity data.

The combination of the clayey nature of the upper unit, relatively saline groundwaters, and abundant salts that can be solublized by rain water and rising groundwaters produce a highly conductive near-surface environment. However, ground conductivity measurements

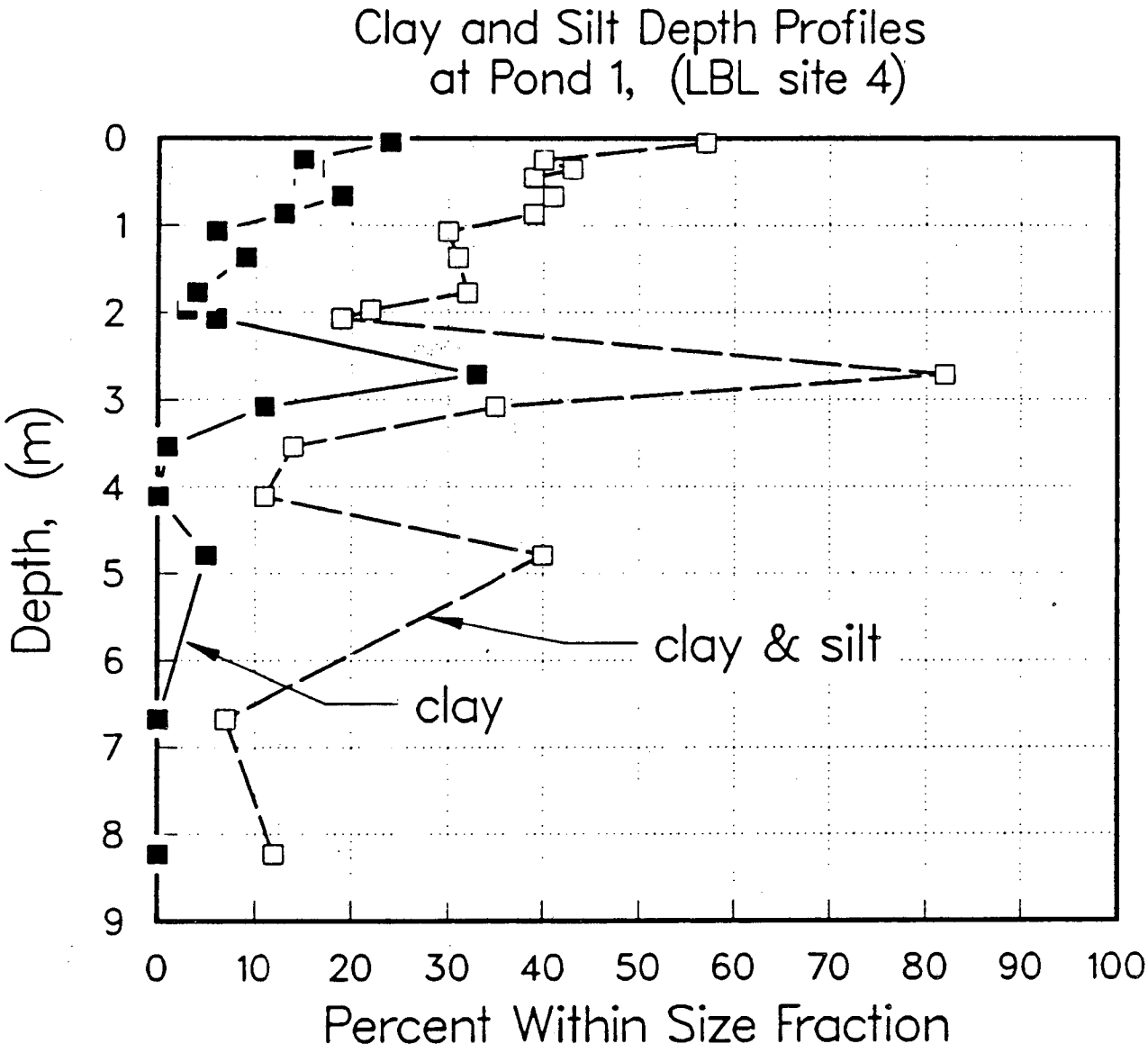

Figure 3. Clay and silt depth distributions beneath Pond 1 (ESD, 1986).

were made in October during the driest time of the year when the saturated zone is at a depth of approximately 2 to 3 m, and the average fluid saturation in the top meter or so was probably about 50-80%. Had the EM surveys been made during the rainy season when the upper unit becomes saturated by the rising groundwaters, the near-surface ground conductivity may have been so high as to make it impossible for us to resolve the conductivity of the lower sandy unit.

The Conductivity Survey Grid and Survey Procedures

The ground conductivity measurements were made along eleven lines trending approximately N60°W true north, plus two shorter cross lines (A–A′ and B–B′) (Figs. 1 and 4). The main lines are roughly parallel to the San Luis Drain where it borders Pond 1 and are 100 m apart. The grid origin, located near a fence intersection close to well KR-47, and the end points of all lines were re-established for the 1988 survey by means of a transit and chain survey.

Readings were taken at 20-m station intervals along all lines. Line orientations were established by means of transit, and stations were located using a 20-m cable used with the EM34 ground conductivity meter. The entire survey covers approximately 2 km^2, excluding the small area occupied by ranch buildings and corrals at the end of Gun Club Road.

At least three conductivity measurements were made at each station to obtain enough information for depth discrimination. At each station one measurement was made with the EM31 (vertical dipole configuration, colinear with the survey line). For greater depths of investigation EM34 readings were taken with intercoil separations of 20 and 40 m[1]. Both EM34 readings were taken using the horizontal dipole configuration in which the coils are placed on the ground with their planes vertical and coplanar; the high near-surface conductivity precluded the use of the vertical dipole configuration. To determine whether anisotropy was a

[1]In this report we will refer to EM34/20 and EM34/40 to indicate EM34 readings with the 20- and 40-m coil separations.

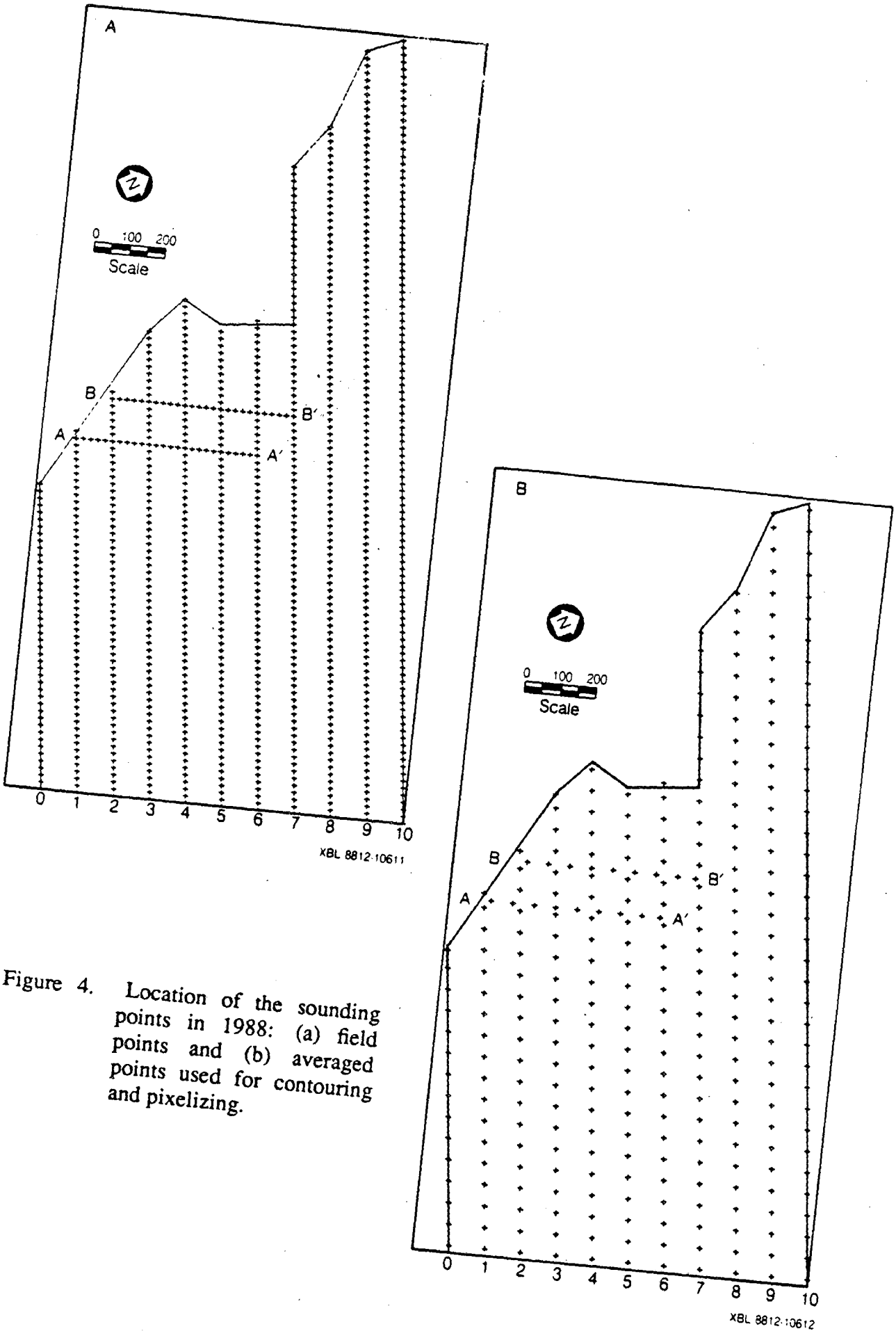

Figure 4. Location of the sounding points in 1988: (a) field points and (b) averaged points used for contouring and pixelizing.

factor, additional readings were taken at many stations after rotating the EM 31 boom 90° aligning it normal to the survey line. In most cases the two readings differed by less than 10 mS/m. As this is within the measurement accuracy of the instruments over very conductive ground we conclude that conductivity anisotropy is not an important consideration.

Brief discussions of the instruments used, technique principles, and data accuracy are given in Appendix A.

Data Reduction and Presentation

Because conductivities throughout the survey area are high, approaching the limit of the low induction number approximation discussed in Appendix A, the instrumental responses departed from linearity between the true and indicated ground conductivities. Consequently, each of the meter readings had to be corrected (McNeill, 1980). Rather than doing this graphically, a slow and laborious process, the corrections were made numerically using a program we developed based on the exact analytical expressions for the EM31 and EM34 meter readings over a homogeneous earth of arbitrary conductivity (Anderson, 1979). The program also accounts for instrument height above ground level; 0.8 m for the EM31 and 0.315 m for the EM34, horizontal dipole mode. The program converts the instrument readings to the apparent conductivity if the earth were uniform at each station.

Figure 4a shows the locations of the sounding points for the 1988 survey, including those along two cross lines, A-A′ and B-B′. To assist in obtaining smoothed contour plots, the corrected meter readings along each survey line were averaged around every third reading. The location of the points used for contouring are shown in Figure 4b. The field and averaged data for line 3 in 1987 are compared in Figure 5. Three-point averaging has a large smoothing affect on the EM31 data which are susceptible to variations in near-surface conditions. Averaging has a much smaller affect on EM34 readings which are already strongly volume averaged.

Figure 6 and 7 show the EM31 isoconductivity contours plotted at contour intervals of 50

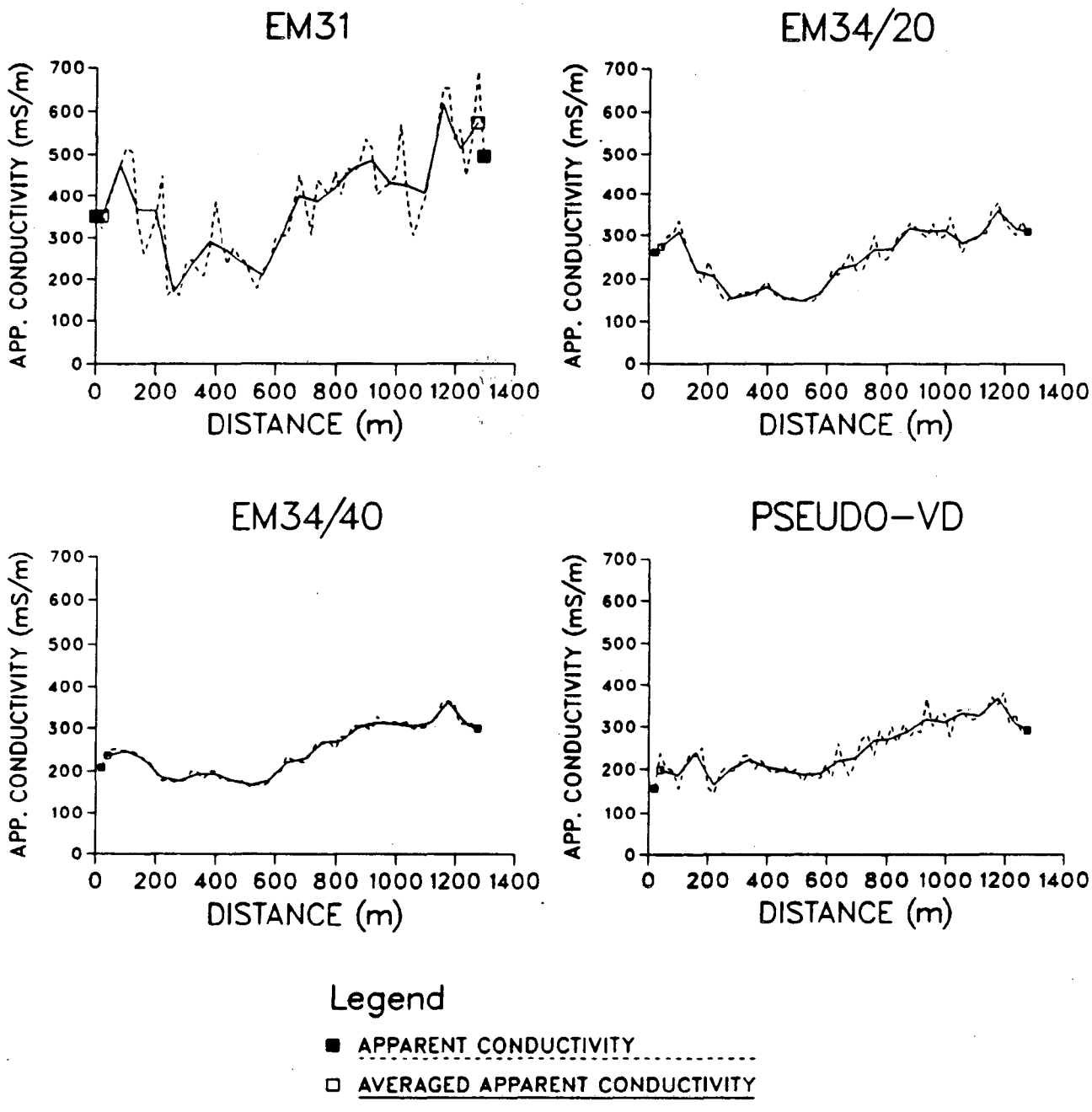

Figure 5. An example of the effect of three-point averaging in smoothing the calculated data. Shown here are the unsmoothed and smoothed apparent conductivities for Line 3, 1987.

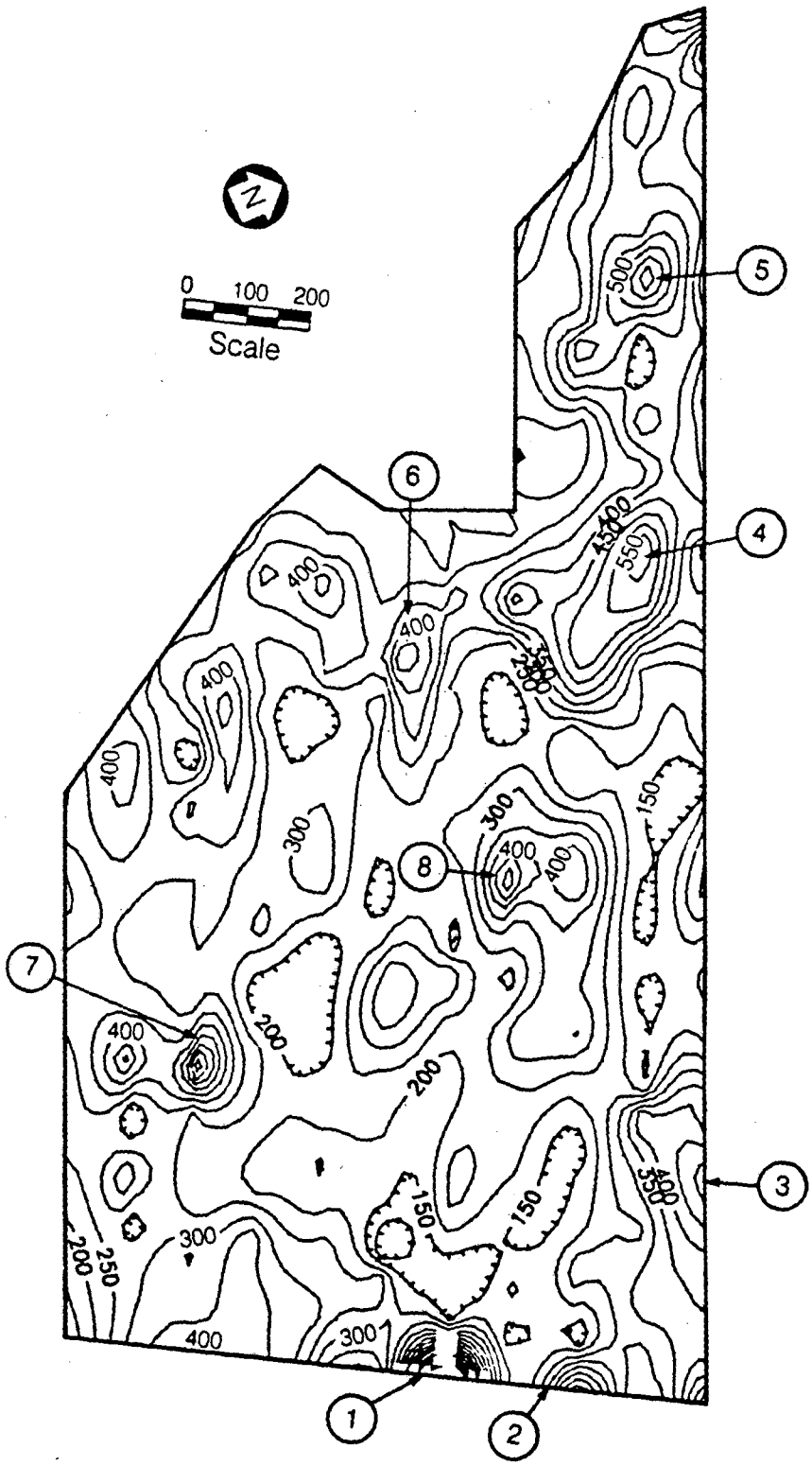

XBL 8812-10610

Figure 6. Isoconductivity contours for 1988 based on measurements with the Geonics EM31. Contour interval is 50 mS/m. The circled numbers refer to discrete conductivity maxima discussed in text.

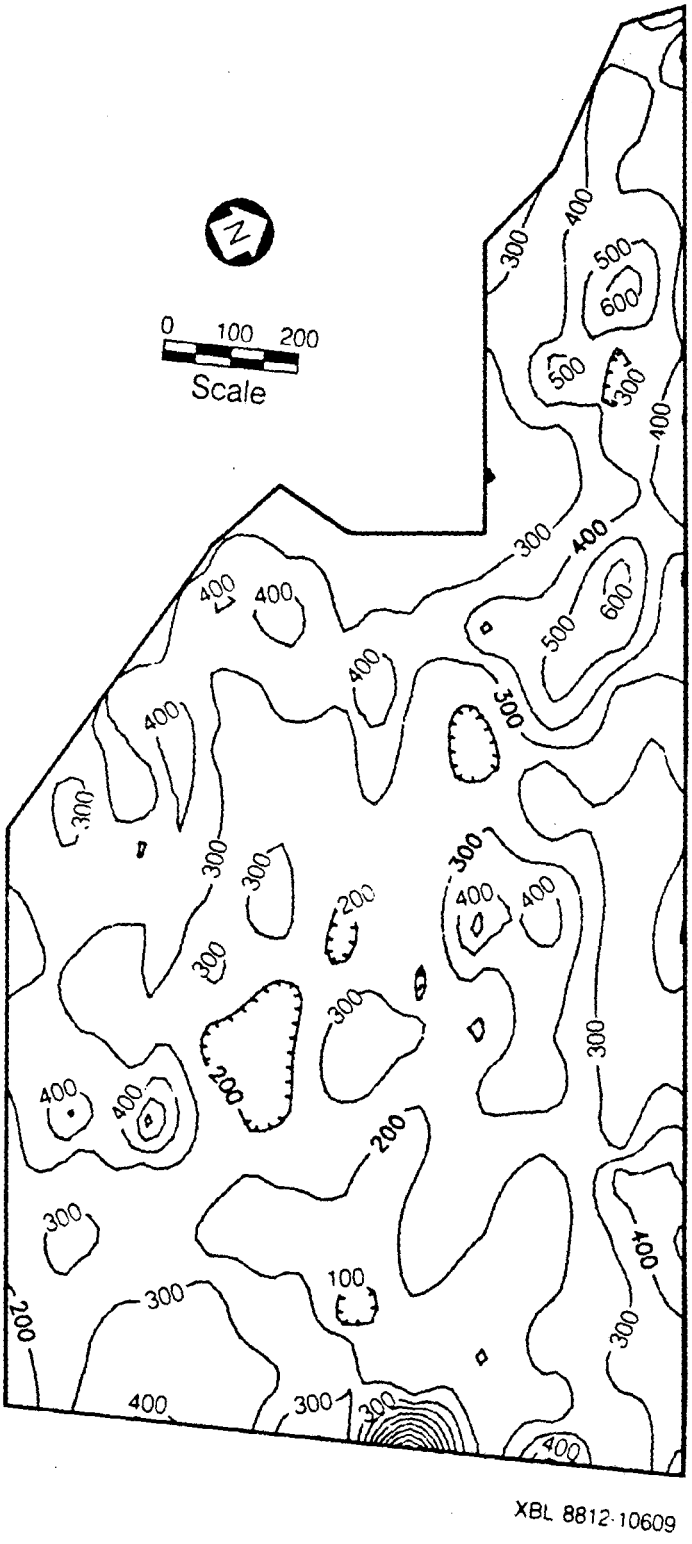

Figure 7. Isoconductivity contours for 1988 based on measurements with the Geonics EM31. Contour interval is 100 mS/m.

and 100 mS/m, respectively.

Figure 8 and 9 show the results for the EM34/20 and EM34/40 surveys, respectively. These data are plotted at a 50 mS/m contour interval.

As indicated by Table 1 of Appendix A, the data plots are presented in order of increasing depth of investigation. Because each progressive plot shown (Fig. 6 through Fig. 9) also involves greater volume averaging of ground conditions, the isoconductivity plots become progressively smoother as they become more strongly influenced by larger volumes of deeper soils and rocks. Nevertheless, both the EM31 and EM34 HD-mode readings are highly sensitive to near-surface conductivities, and these may mask the effects of deeper variations.

To overcome this problem, a simple procedure was followed which, in effect, transforms the EM34 depth-response function to one less sensitive to the near-surface conductivity (McNeill, 1985). The procedure is to calculate a new apparent ground conductivity (σ_{an}) at each station;

$$\sigma_{an} = 2\sigma_{40} - \sigma_{20}$$

where σ_{40} and σ_{20} are the apparent conductivities at the 40- and 20-m intercoil spacings, respectively. This operation alters the effective depth-response function to one that has zero sensitivity at the surface and maximum sensitivity to conditions at depths of about 0.25 times the larger intercoil separation (Appendix A, Fig. A.2). The resulting ground conductivity map (Fig. 10) de-emphasizes the high and variable conductivities near the surface and gives more weight to conductivities within the saturated zone. Because Figure 10 is theoretically similar to what would have been measured directly had it been possible to use the vertical dipole (VD) mode of operation, we refer to the display in Figure 10 as a Pseudo-VD isoconductivity map.

Significant anomalies compiled from conductivity data at all depths and from the Pseudo-VD data are shown in Figure 11.

In addition to preparing the isoconductivity contour maps, the ground conductivity data for years 1987 and 1988 are shown as a series of "pixel" plots in Figures 12 through 15.

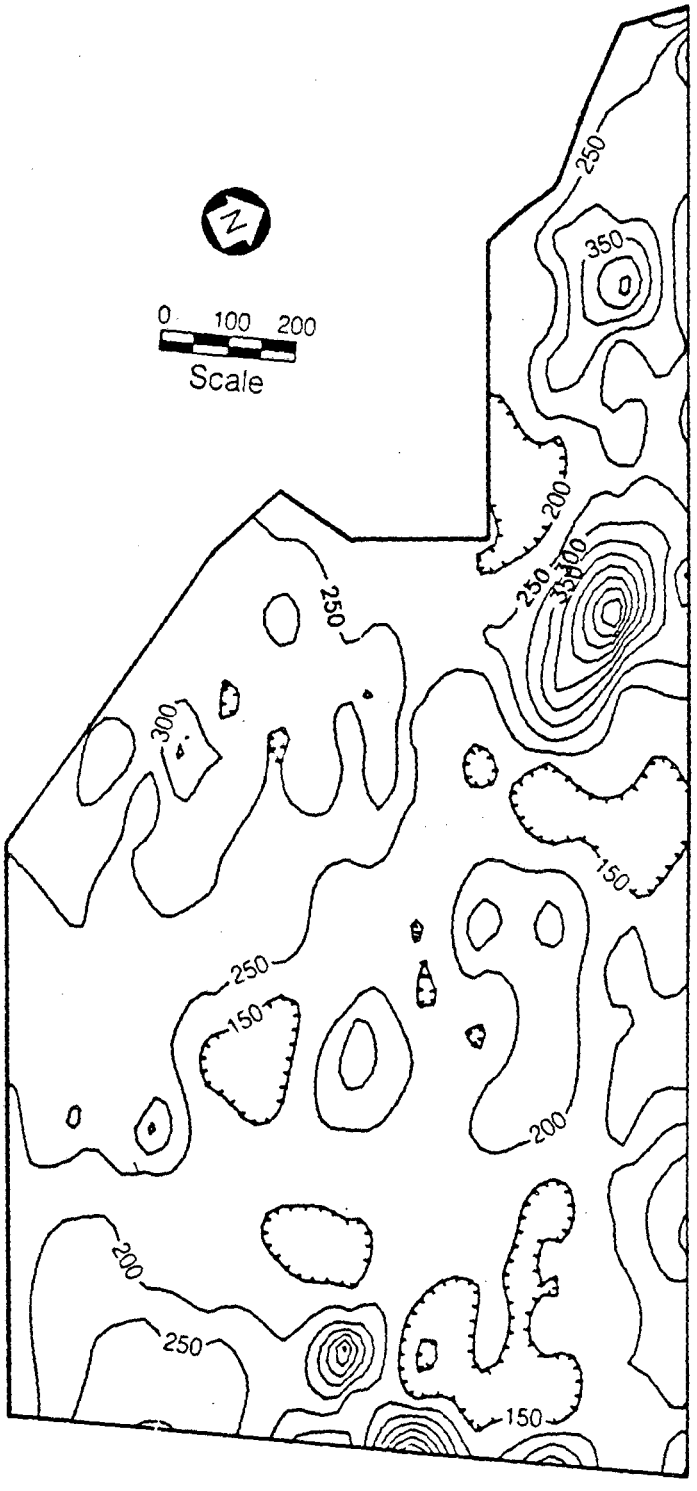

Figure 8. Isoconductivity contours for 1988 based on measurements with the Geonics EM34 with a 20-m intercoil separation. Contour interval is 50 mS/m.

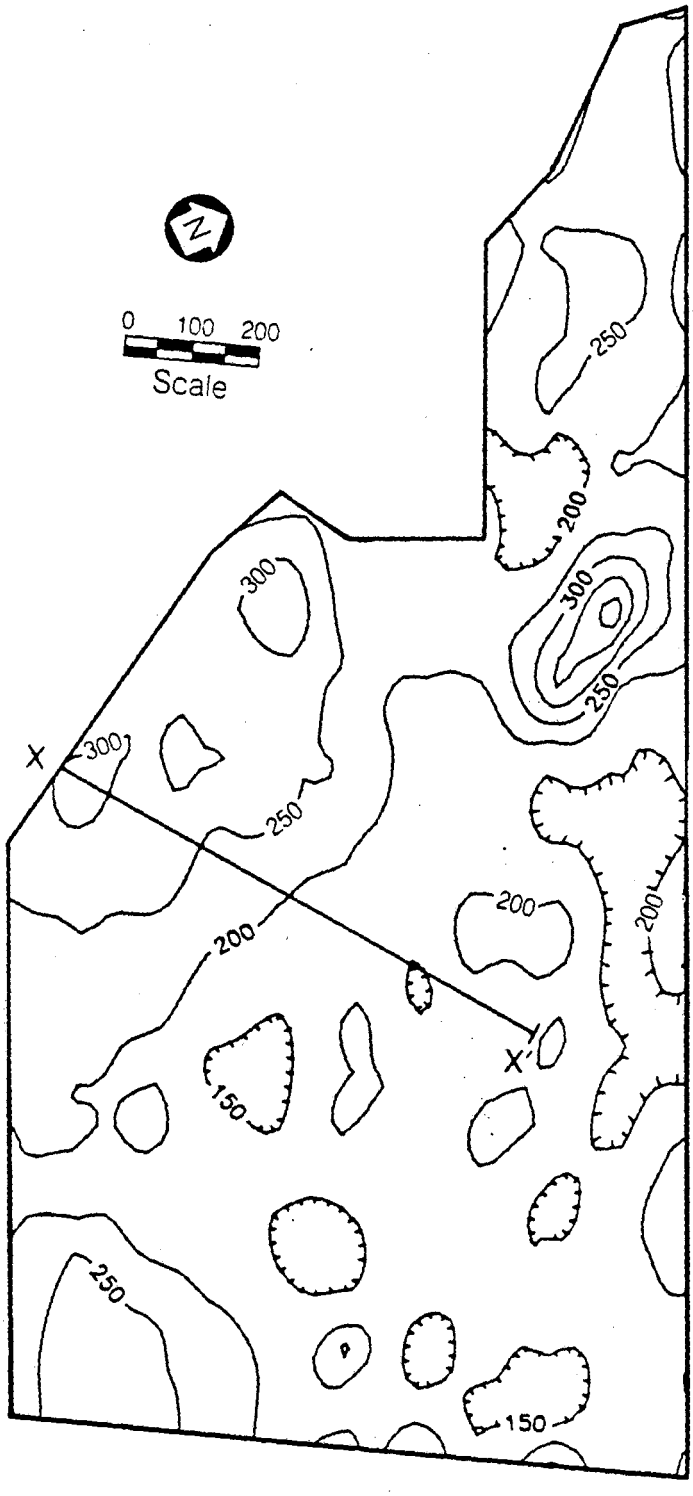

Figure 9. Isoconductivity contours for 1988 based on measurements with the Geonics EM34 with a 40-m intercoil separation. Contour interval is 50 mS/m.

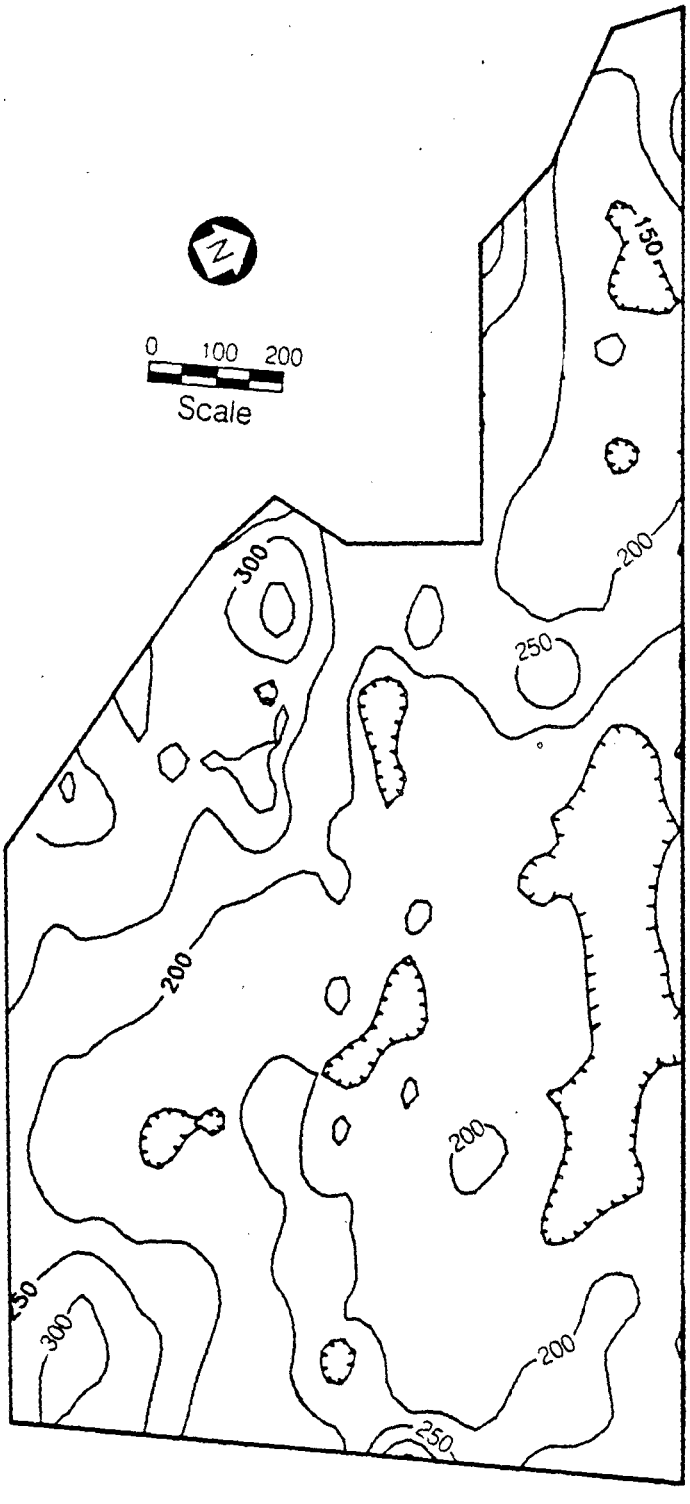

Figure 10. Isoconductivity contours for the 1988 computed Pseudo-VD model. Contour interval is 50 mS/m.

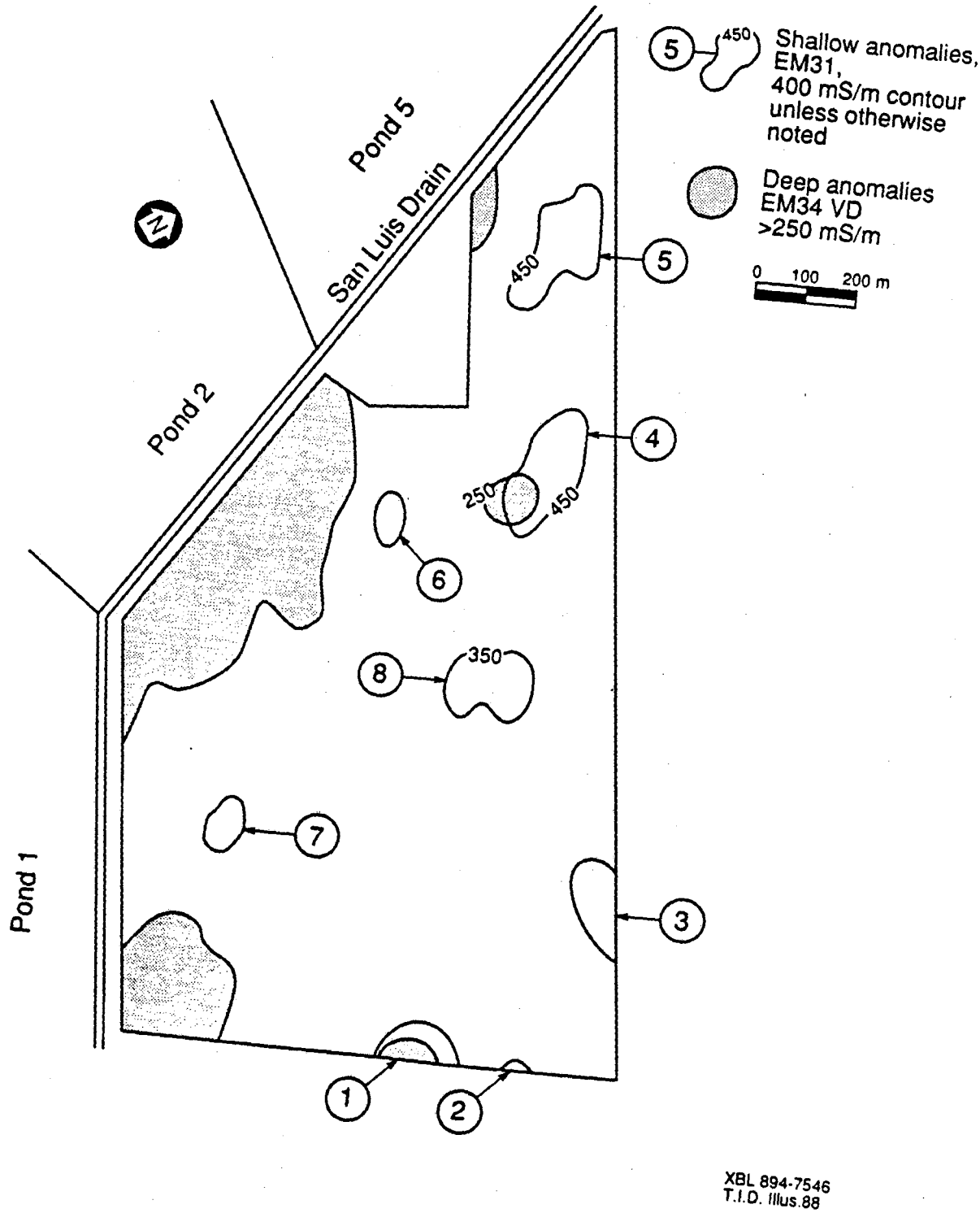

Figure 11. Anomalous subregions of the survey area discussed in the text.

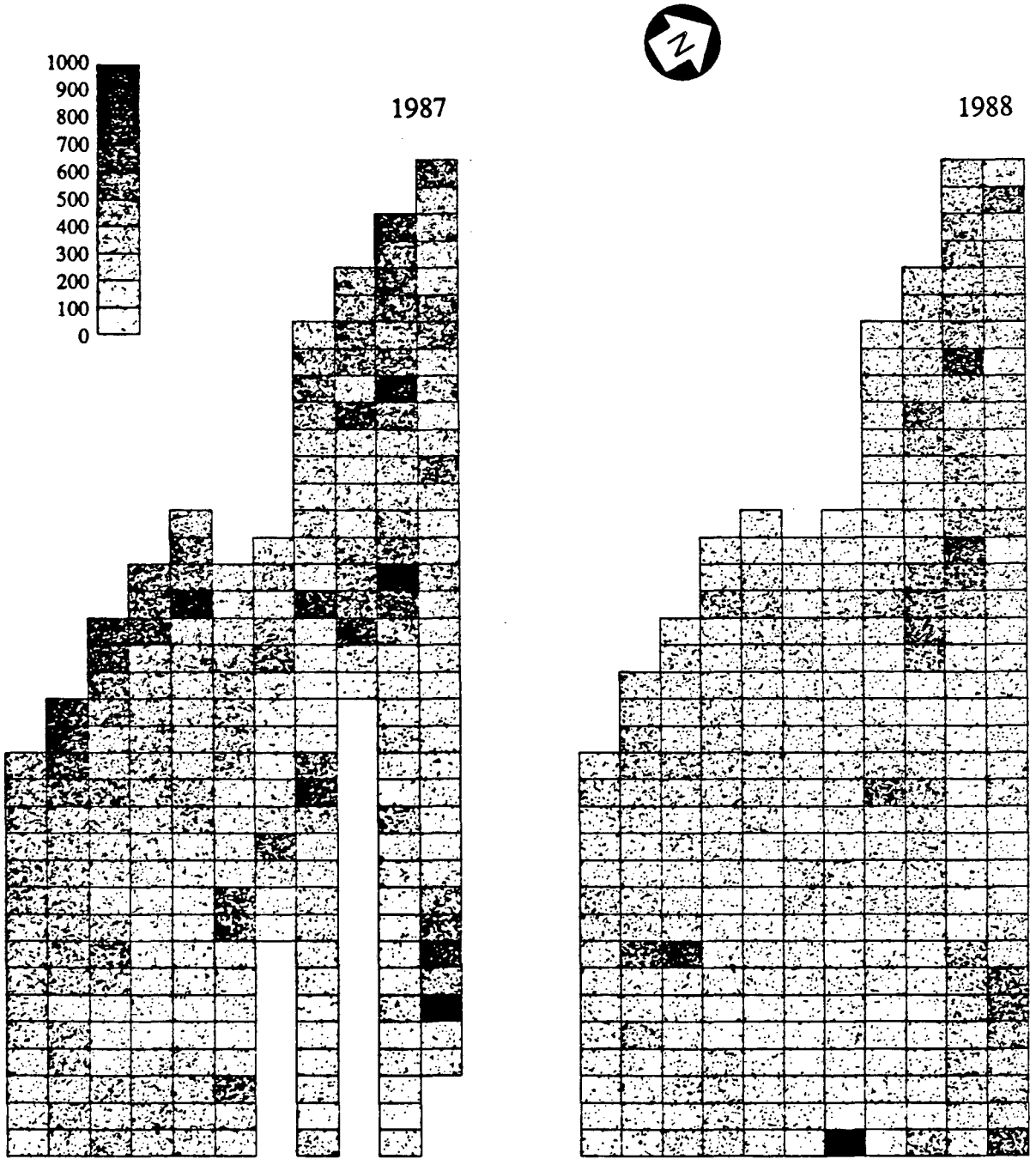

Figure 12. Pixel diagrams showing the comparison between the 1987 and 1988 apparent conductivities for the EM31. Each rectangle represents an area of 100 by 60 m.

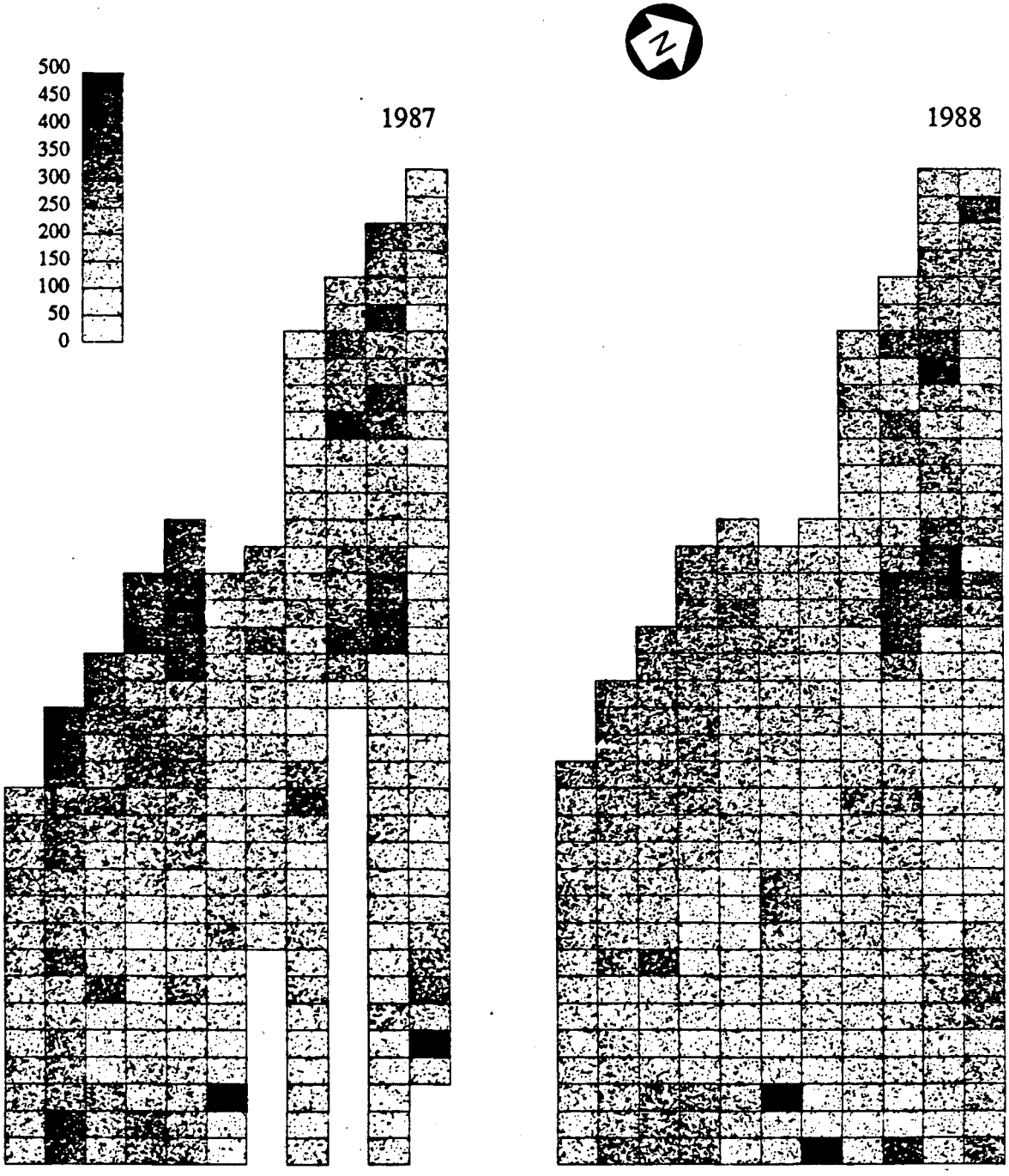

Figure 13. Pixel diagrams showing the comparison between the 1987 and 1988 apparent conductivities for the EM34/20. Each rectangle represents an area of 100 by 60 m.

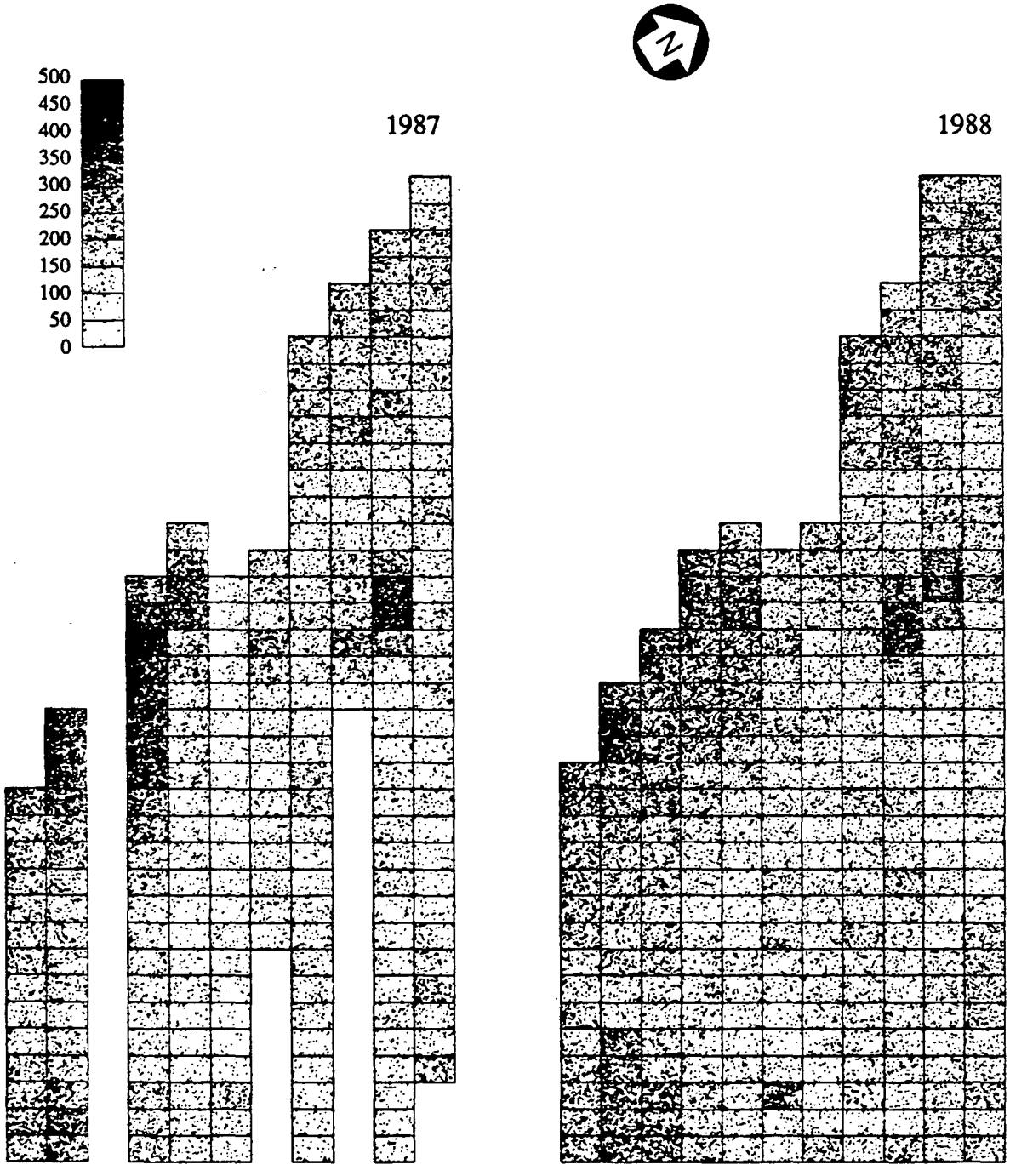

Figure 14. Pixel diagrams showing the comparison between the 1987 and 1988 apparent conductivities for the EM34/40. Each rectangle represents an area of 100 by 60 m.

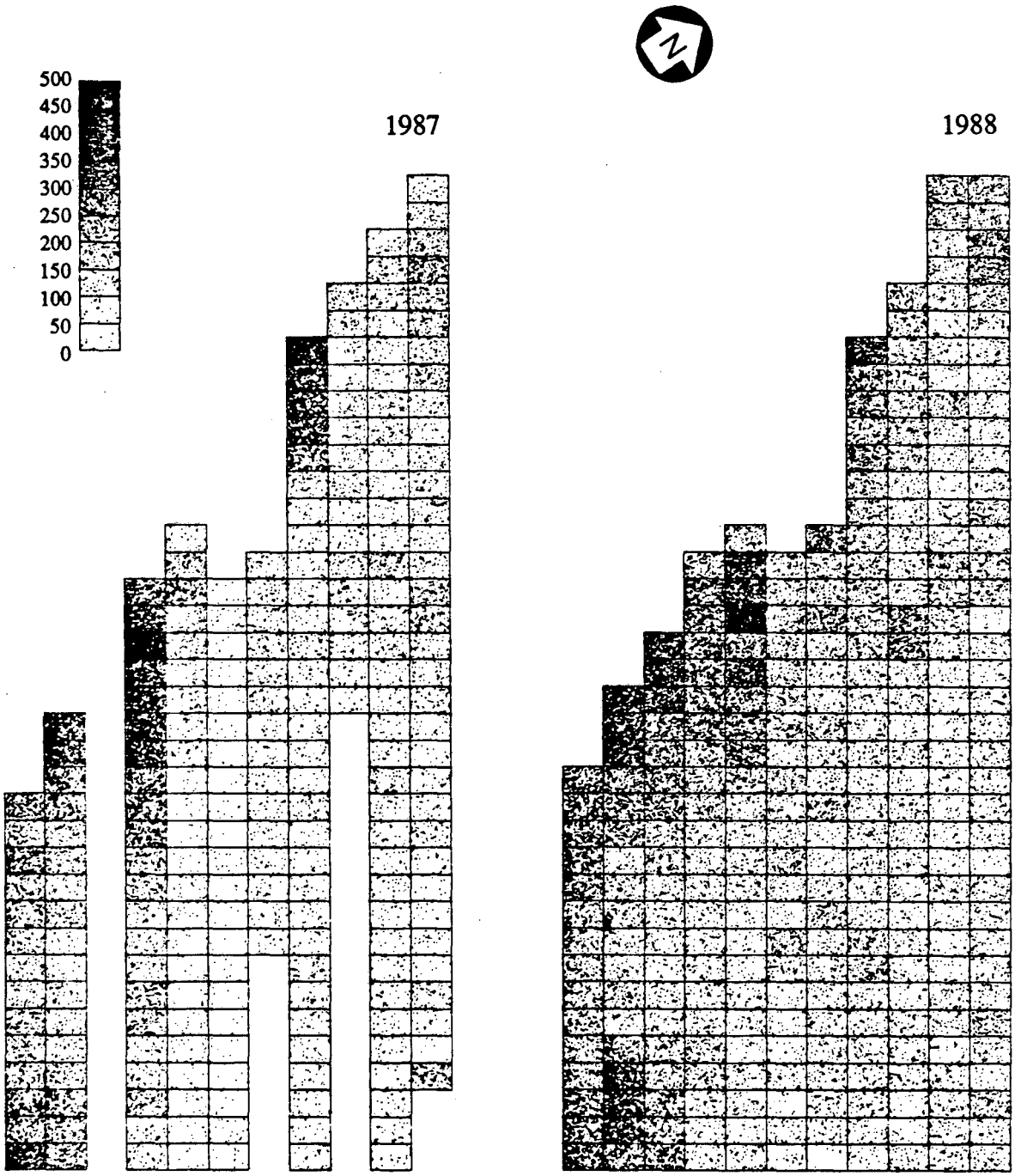

Figure 15. Pixel diagrams showing the comparison between the 1987 and 1988 calculated apparent conductivities for the Pseudo-VD. Each rectangle represents an area of 100 by 60 m.

Averaged apparent ground conductivity values calculated for the contour plots are displayed as rectangular regions in which the dot (or speckle) density is directly proportional to the apparent ground conductivity. The program divides the range of conductivities into 10 equal parts, and assigns a proportional dot density to each.

Discussion of Results

Isoconductivity Contour Maps

Figures 6 and 7 show the EM31 results contoured at 50 and 100 mS/m intervals, respectively. These plots indicate the high apparent conductivity of the upper lithologic unit, and its highly variable nature over the Fremont Ranch. The apparent conductivities average around 300 to 400 mS/m, and several isolated highs exceed 600 mS/m. There appears to be no correlation between apparent conductivity values measured with the EM31 and proximity to the Kesterson Ponds. However, correlations can be made between most of the major maxima and features discernible on color aerial photographs. Photographs taken during the winter months of 1988 when grasses were growing give the best color contrast results.

The main features in the EM34 figures (Figs. 7, 8, and 9) are broad highs adjacent to the ponds. Most of the isolated maxima present in the EM31 data are not present in the EM34 readings, due mainly to the greater volume averaging that occurs as coil separation is increased and transmitter frequency is decreased. In the EM34/40 readings the only maxima remaining are those numbered 1 and 4 in Figure 6. These may be due to conductive features with greater depth extent than the others.

To accentuate conductivity variations within the lower lithologic unit, a pseudo vertical-dipole map was generated using the algorithm described in a previous section (Fig. 10). The highest values of apparent conductivity (300 to 350 mS/m) border the Kesterson Ponds. The most significant feature on the figure is a broad, irregular high adjacent to Pond 2. A smaller high occurs adjacent to Pond 1, and a suggestion of a high exists adjacent to Pond 5.

Anomalous areas numbered 1, 2 and 3 in Figure 11 all correlate with larger and distinct

natural drainage features. Peak 1 lies in the depression of a large, arcuate ox-bow lake, a relict feature of the meandering San Joaquin River drainage system. Peaks 2 and 3 are associated with a modern slough which drains into Salt Slough.

On the other hand, peaks numbered 4 through 8 correlate with small color anomalies on the aerial photographs, areas that do not acquire a normal grass cover. Of these maxima, 4 and 5 are associated with bleached areas; the others with dark-colored, presumably muddy, depressions. A field check in March 1989 confirmed extensive bleaching in the area of peak 5.

Comparisons of 1987 and 1988 Data

Variable dot-density pixel plots were computer constructed to provide a simple means for comparing the 1987-1988 data. The EM31 results are shown in Figure 12, where the ten density levels span the 0 to 1000 mS/m conductivity range. In general, one observes that a general decrease in EM31 ground conductivity has occurred between 1987 and 1988. This is most likely due to drier soil conditions and a drop in the water table elevation. Additional discussion on these points is provided in the section on sensitivity analyses.

The EM34 results are shown in Figures 13 and 14; the Pseudo-VD are shown in Figure 15. The ten dot-density levels here span the range of 0 to 500 mS/m. The Line 2, 1987 measurements have been removed from the EM34/40 and Pseudo-VD figures, as these data were affected by a weak transmitter battery. This condition gave readings which appeared to be genuine, but which in fact are biased either higher or lower, in no predictable fashion (F. Snelgrove, 1989; personal communication). As there was no way to correct for this problem, the questionable data were simply discarded. For the 20-m coil separation sounding, the 1988 EM34 results show a more uniform (overall) conductivity, and lower values near the ponds compared to 1987. The values for the 1988 40-meter separation data also seem to be more uniform and slightly higher away from the ponds.

As with the isoconductivity contours, the most significant features in these pixel figures are the high ground conductivities adjacent to the ponds. Based on their location, shape, and magnitude these anomalies appear to be caused by infiltration and migration of the agricultural

drainwater used to flood the ponds between 1981 and 1986. Adjacent to Pond 2 the anomaly is well defined for all depths of investigation. From the 1987 and 1988 EM34/20 and EM34/40 data the maximum lateral extent of migration appears to be 300 m from the fence-line of the Fremont Ranch. Next to Pond 1 the anomaly is well defined only for the larger depths of investigation, and it appears to extend 200 m. Next to Pond 5 the anomaly is best seen in the Pseudo-VD figure. It appears only along Line 7, indicating a very limited extent of migration.

Changes in the shape and location of this plume are illustrated best by EM34/40 data (Fig. 14). Adjacent to Pond 2, the conductivity readings have decreased slightly on Line 3, and increased slightly along Line 4. This pattern is consistent with intermingling between the fresher water used to flood the ponds during 1986-1987 and the saline drainage water plume. However, it is difficult to definitively conclude whether the observed changes are due to infiltration and migration of fresher water because no data are available from Line 2, where the changes should have been most noticeable. A similar pattern is apparent adjacent to Pond 1; however, even the 1987 data indicated that fresher water may have already migrated as much as 100 m. Only slight differences are seen next to Pond 5. Although the pattern of changes in conductivity data are consistent with slight migration of the plume, we could not detect migration of the leading edge of the plume. This is most likely due to the coarse spacing of the survey lines, which is not adequate to detect migration for an estimated flow rate of 5 to 50 m/year (Benson, 1988).

Inverse Modeling

As another means of analyzing and comparing the 1987 and 1988 data sets, 1-D numerical inversions were run for data along a long profile line, X-X′ (see Fig. 9) which crosses the ground conductivity anomaly adjacent to Pond 2. Although the isoconductivity contour maps indicate that ground conductivity does not appear to be uniformly layered (or 1-D) over large areas, the pieced-together 1-D inversions should, nevertheless, provide the basis for informative comparisons. Two- and three-layer 1-D fits to the combined EM31 and EM34 meter readings

were made using PC program EMIX34 developed by Interpex Corporation of Golden, Colorado. EMIX34 uses a ridge regression technique to find the best least-squares fit to the meter readings. Given the three meter readings, the program iterates to find the best two-layer fit (conductivity and thickness of the first layer and conductivity of the underlying layer) to the data. By constraining second layer thickness and third layer conductivity, the program was also used to solve for the layer parameters in a three-layer earth model.

The program ran 12 iterations, displaying the percent residual error between the actual and calculated readings after each iteration. In only a few cases the residual error had not converged within these iterations. For these cases the data sets were rerun using the final model from the first run as the initial model for the second. The poor convergence was probably due mainly to near-surface geologic effects such as lateral heterogeneities. For this reason inversions were also run using meter readings averaged for sets of two or three adjacent stations. The two approaches often gave different results, and judgment was needed to select which of results were plotted in the conductivity sections.

As discussed before, the EM34/40 1987 readings on Line 2 were discarded because of low battery strength during measurement. Inverting this data set required fixing one parameter. On the basis of the adjacent inversions, the first layer thickness (h_1) was set at 1 meter. The resulting two-layer inversion gives a very small least-squares residual error (0.5%), but because only two data points were used, the actual error in conductivities σ_1, σ_2 and thickness h_1 could be much larger.

The two-layer conductivity models for 1987 and 1988 are shown in Figure 16. Layer conductivities are given in mS/m, the first layer thicknesses are indicated by the horizontal bars, and the percent residual errors in the least-square fits are shown in brackets. The letter F indicates a "fixed" parameter. Two significant differences between the two years stand out. First, an increase in first thickness (h_1) and decrease in first layer conductivity (σ_1) are seen at most points for the 1988 data compared to the 1987 data. This can be attributed to a lower soil moisture and a deeper saturated zone. Second, a slight reduction in second layer conduc-

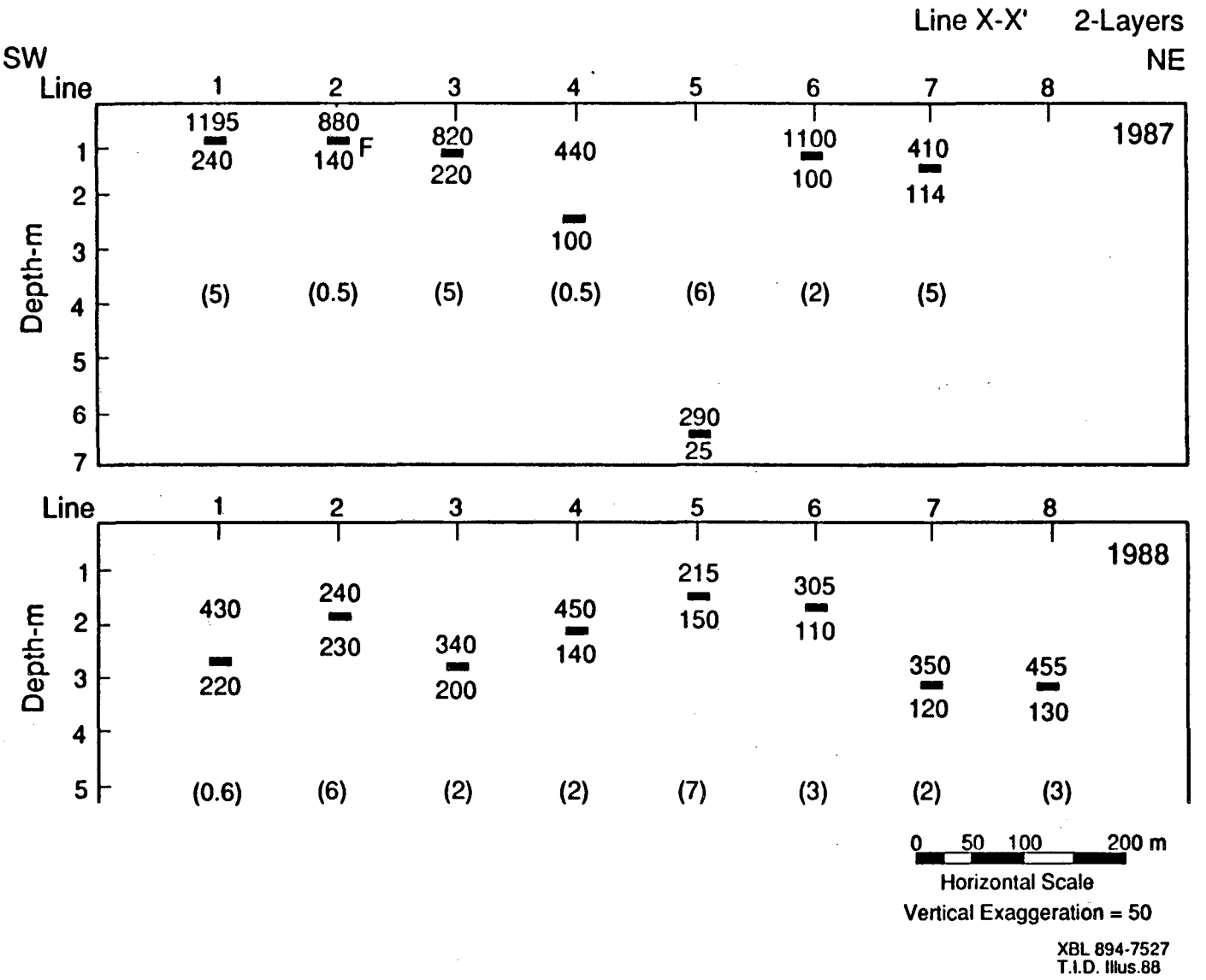

Figure 16. Comparison of the 1-D two-layer inversions of the 1987 and 1988 meter readings along Line X–X′ (Fig. 9). First layer depth is indicated by the horizontal bar, layer conductivities are given in mS/m, and the residual errors in the least-squares fit are shown in percent within brackets. F signifies a fixed parameter.

tivity (σ_2) near Pond 2 (Lines 1 and 3) is observed, and a slight increase in σ_2 farther from the pond (Line 4). Together, these changes in σ_2 suggest that the saline groundwater in the sandy-arkosic lower unit near Pond 2 may have been displaced by fresher groundwater and its leading edge may have migrated eastward. However, we do not have enough confidence in the inversion accuracy to definitively conclude that this has occurred. The 1-D results at Line 5, 1987, are so different from the adjacent lines that we question their accuracy. We believe that EM34/40 readings taken on Line 5 in 1987 may also be inaccurate due to operator error.

Figure 17 shows the results after the same data are inverted assuming a three-layer model. For these calculations the thickness h_2 of the sandy shallow aquifer was fixed at 17 m and the conductivity of the substratum, σ_3, was fixed at 100 mS/m. A strong similarity exists between the two- and three-layer model results, particularly for the 1988 data. This indicates that parameters h_2 and σ_3 have only a weak influence on the ground conductivity measurements. Stated another way, the high conductivities near the surface result in a high attenuation of the EM fields generated by the EM31 and EM34 so that parameters h_2 and σ_3 cannot be resolved (see Appendix A).

Accuracy of the 1-D Inversions

The accuracy of a 1-D inversion depends on several factors; foremost among them are geologic noise caused by proximity to a lateral discontinuity (e.g., a surface conductivity inhomogeneity), noisy data, and equivalence behavior. The latter comes out of the physics of the electromagnetic method, and bears on the question of how well layer parameters can be resolved by means of the currents induced in the earth. The 1-D inversions show that the fundamental conductivity stratification beneath the survey area is classified as an A-type; i.e., conductivity decreases with depth. Numerical tests for A-type and other models made by Fitterman et al. (1988) show that the quadrature frequency-domain EM (FEM) measurements, as made by means of the EM31 and EM34 instruments, share a general problem with other sounding methods under A-type conditions. First, the three-layer 1-D inversions are sensitive to the the conductance of the second layer (the product of second layer conductivity σ_2 and

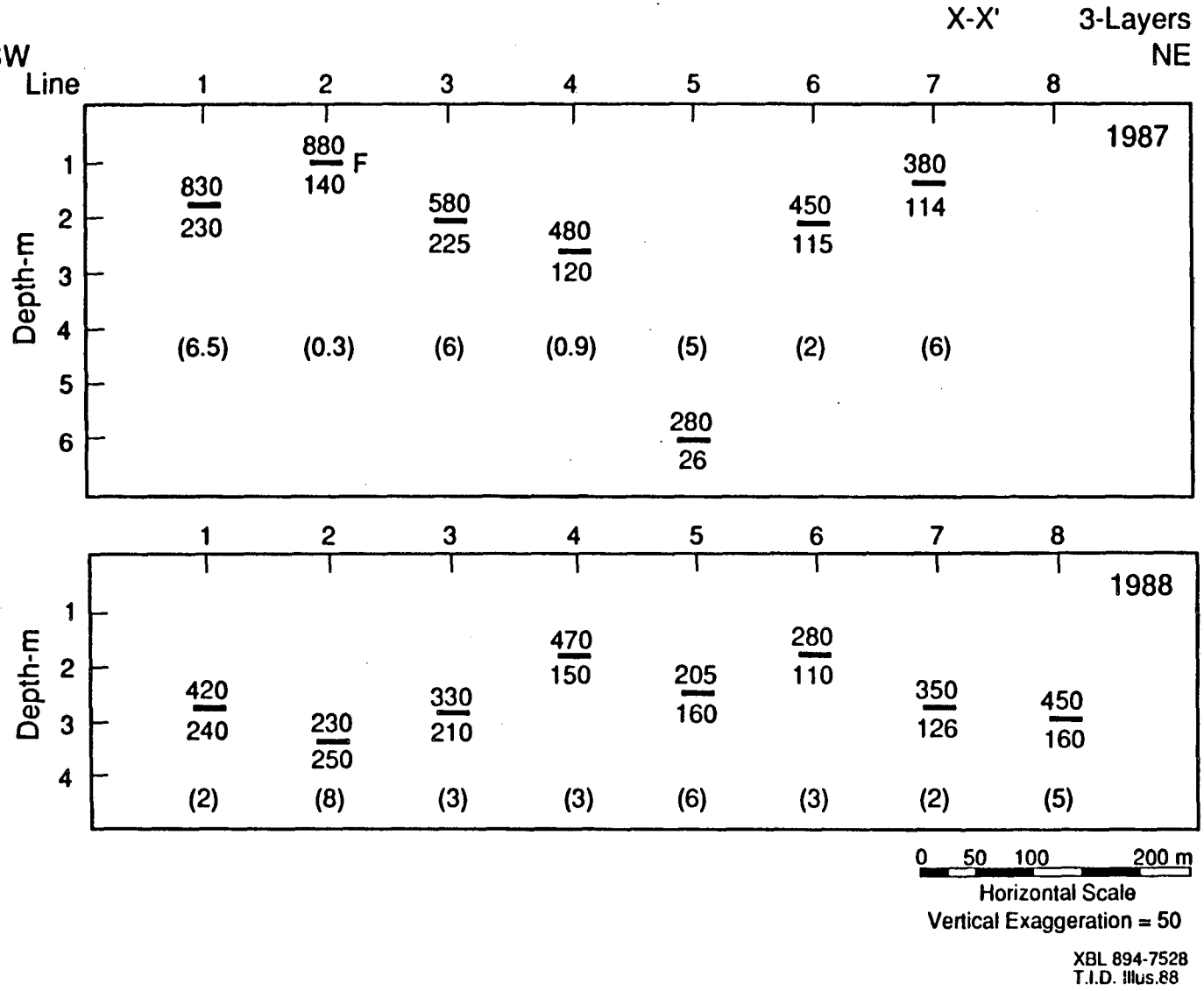

Figure 17. Comparison of 1-D three-layer inversions of the 1987 and 1988 meter readings along Line X–X′ (Fig. 9). For these inversions of the second layer thickness was fixed at 17 m and the third layer conductivity was fixed at 100 mS/m.

thickness h_2), but neither σ_2 nor h_2 is individually well-resolved. Second, there is poor resolution of the transition from first to third layer. This problem (called suppression) says that a two-layer model will fit the data as well as a three-layer model; i.e., the effect of the second layer is suppressed and it is difficult to distinguish.

Neither of these two physical problems applies to the measurements made over the Fremont Ranch. Because the EM responses approximate those for a simple two-layer earth the problems of middle layer equivalence and suppression do not appear to be important. The major source of inaccuracy in the 1-D models, then, appears due to lateral variability in the near-surface conductivity, which as seen in Figure 5 corresponds to changes (after smoothing) on the order of 10-25% over distances as small as 20 m.

Data Averaging

To look for systematic differences in the 1987 and 1988 data sets, the apparent conductivities along each line were averaged for each of the three meter readings and for the Pseudo-VD conductivities.

Data from only the first 860 m of each line were used so that all the points along each line would be approximately equidistant from the edge of the reservoir. Figure 18 shows the mean values, and the 95% confidence intervals for each of the four data sets.[2] Averages values that are significantly different between the two years are indicated by an asterisk.[3] For both years all three instruments give higher average readings out to 300 m, suggesting that this marks the average migration of the leading edge of the drainage water plume.

---

[2]The upper and lower limits for each mean were calculated for a 95% confidence level ($\alpha = 0.05$) by: $\bar{y} \pm (Z_{\alpha/2}\sigma)/(n^{1/2})$ where $\bar{y}$ is the mean of the data, σ the standard deviation of the mean, n the number of data points, and $Z_{\alpha/2}$ the area under the normal distribution curve bounded by $\pm Z_{\alpha/2}$ such that $(1 - \alpha)$% of the samples fall into the bounded region (Mendenhall, 1975). For a 95% confidence level $Z_{\alpha/2} = 1.96$. When less than 30 data points were available, the students' t distribution was used as the test statistic, as is appropriate for smaller sample sizes. This corresponds to using $T_{\alpha/2}$, instead of $Z_{\alpha/2}$. For $\alpha = 0.95$, $T_{\alpha/2} = 2.11$.

[3]Mean values are judged to be significantly different at the 95% confidence level if $(\bar{y}_1 - \bar{y}_2)/[(\sigma_1^2/n_1) + (\sigma_2^2/n_2)] \geq Z_{\alpha/2}$ (Mendenhall, 1975). Once again, when less than 30 data points were available $T_{\alpha/2}$ was used.

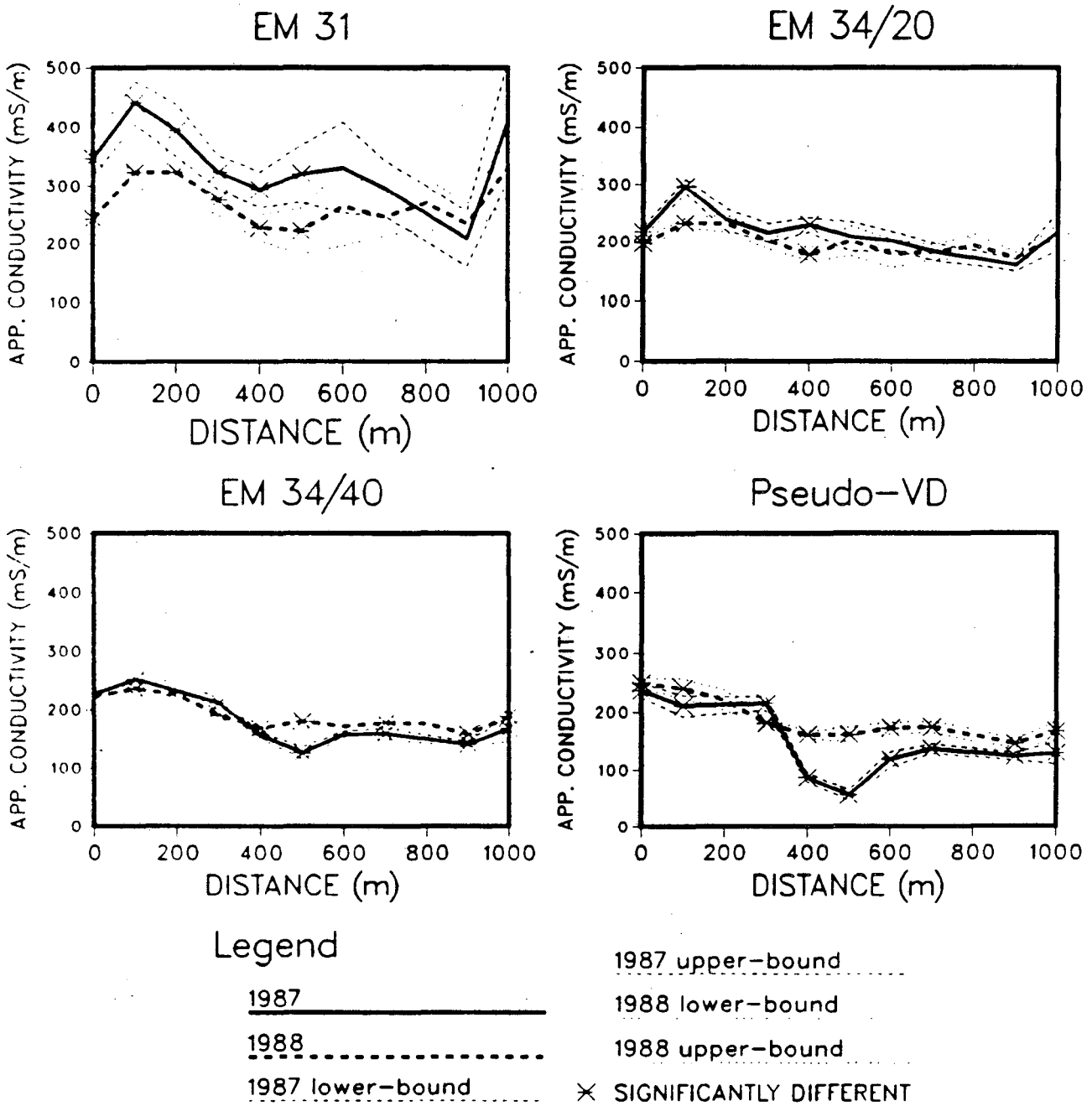

Figure 18. Graphs illustrating the results of the statistical analysis of the apparent conductivity data. The solid line shows the mean values for Lines 0-10 and the envelopes show the 95% confidence limits of the mean. The starred points refer to averages that are significantly different at the 95% confidence level. Note that only the first 860 m of each line is used to calculate the average apparent conductivities.

For lines nearest the San Luis Drain significant differences occur in both EM31 and EM34/20 ground conductivities. A difference in the EM31 averages is apparent out to 600 m from the drain. The EM34/20 is different to only 200 m. Farther away from the San Luis Drain both instruments show similar readings for the two years. As discussed in the following section, the lower EM31 and EM34/20 apparent conductivities near the ponds in 1988 can be accounted for by a combination of a lower water table and lower average saturation in the unsaturated zone.

The statistical analysis of the EM34/40 readings indicates that the values have small but significant differences on all lines except Line 0, which is closest to Ponds 1 and 2. Similarly, the Pseudo-VD averages appear to be significantly different for all lines with large unexplained differences on Lines 4, 5, 6 and 7. We believe that these differences are largely an artifact of the numerical algorithm (for the Pseudo-VD data) coupled with some type of systematic error, rather than the result of physical change in subsurface conditions.

Our belief stems from the fact that confidence levels were calculated on the basis of the spatial variability of the apparent conductivities alone. In doing this it was assumed that all the measurement errors were randomly distributed, and so did not bias the mean value of the sample distribution. In actuality, there are several sources of systematic errors that may bias the mean. For example, one possible source of non-random, systematic error was that the same types but not the same exact instruments were used in the successive surveys. According to Geonics, two units of the same instrument, each properly calibrated, can give readings that are as much as 10% different in a resistive environment. Although no figures are published, it is believed that this source of error may increase in a highly conductive environment. All possible causes of instrument error are reviewed in the Appendix. The cumulative instrument error was calculated to be ±18 mS/m. Consequently, we believe that some of the small but statistically significant differences, such as the 10-20 mS/m differences in the EM34/40 data (see Fig. 18), may be caused by this instrument error. As such, we do not consider these to be significant differences.

Sensitivity Analyses

A set of numerical forward experiments were done to estimate the magnitude of ground conductivity changes that could interfere with the detection of saline plume migration. In this section we discuss the sensitivity of meter readings to various effects encountered in the field: water table fluctuations, rainfall, height of the EM31 above the ground, and salt distribution in the soil. For the calculations Program PCLOOP, Version 1.0, written for an IBM PC and supplied to us by Geonics was used. The program, based on EMLOOPS (Anderson, 1979), calculates the EM31 and EM34 instrument readings for an arbitrary layered earth where layer conductivities and thicknesses are specified by the user. For these sensitivity studies, an extensive literature search was undertaken to find an appropriate empirical expression to describe the bulk conductivity of a sandy soil for a given saturation, porosity, and interstitial water conductivity. No data were available for San Joaquin Valley soils, therefore the conventional Archie's law expression for non-shaley sandstones was used,

$$\sigma_B = a\ \sigma_w\ \phi^m\ S^2, \qquad (1)$$

where σ_B = bulk conductivity of the ground, σ_w = conductivity of the interstitial water, ϕ = porosity, m = the consolidation factor, and S = saturation. The parameters a and m are determined from laboratory measurements and depend on the nature of the sediments. For these studies we chose a = 0.88 and m = 1.37 based on data available for similar sediments tabulated by Keller and Frischknecht (1966). The porosity ϕ was set at 35%, based on analyses of the soils and sediments at Kesterson Reservoir (ESD, 1987).

For these sensitivity studies, the local hydrogeology (Fig. 19) was represented by two general models. The layer thicknesses and conductivity distributions used in the sensitivity studies are shown in Figure 20. The base model (Fig. 20a) has three layers: (1) an unsaturated saline surface layer, (2) a highly conductive saturated saline layer, and (3) a minimally conductive sandy aquifer. To represent the presence of the saline plume, another conductive layer at a depth of 3 to 20 m was added to the base model (Fig. 20b).

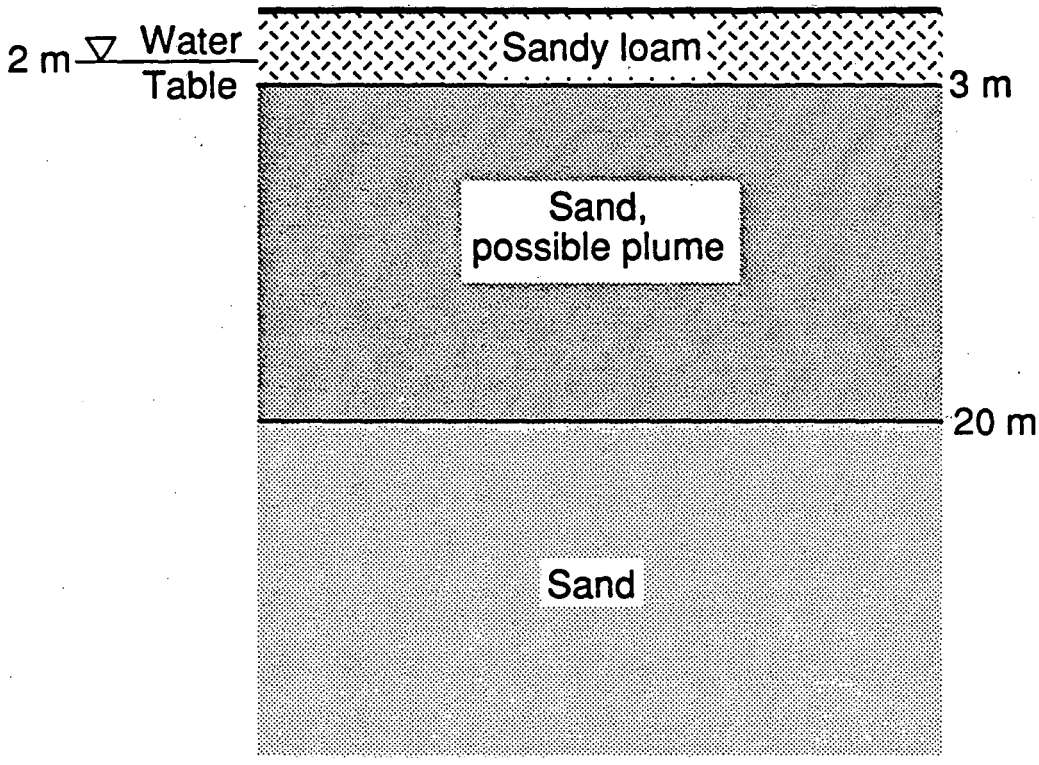

Figure 19. A schematic of the hydrogeology at the survey location used in numerical modeling.

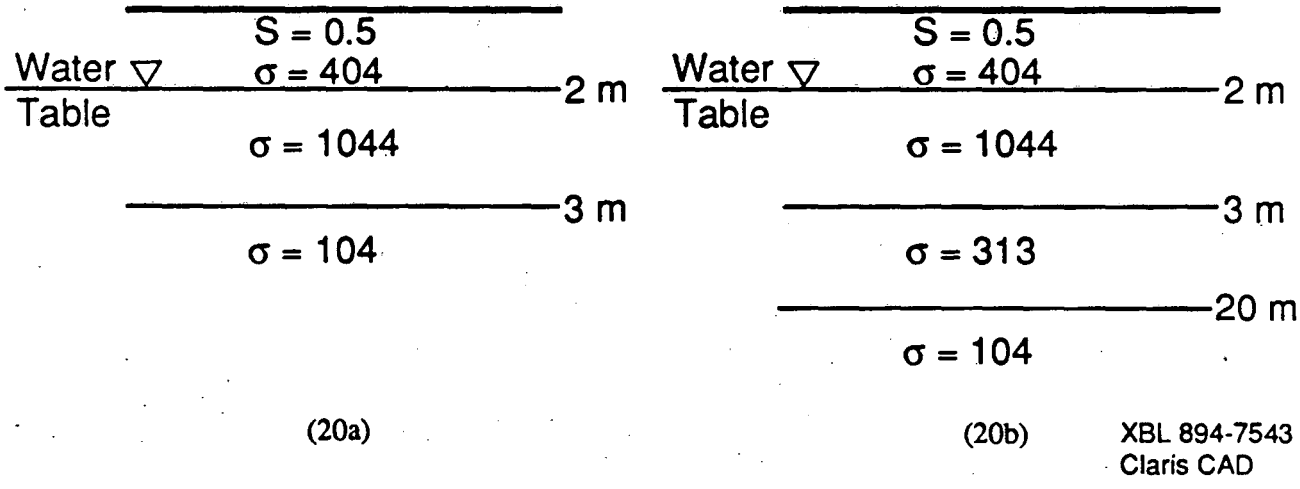

Figure 20. Standard models used in forward calculations (a) without and (b) with the infiltrating plume, where S = saturation and σ = bulk rock conductivity. Note that the first two layers correspond to the sandy loam unit. The models are not drawn to scale.

Water Table Depth

The cessation of flooding the ponds in 1987 caused a drop in the water table immediately adjacent to Kesterson Reservoir between the autumns of 1987 and 1988. Water level data from several wells are shown in Figure 21. Observation wells KR-19, KR-20, KR-47, WQ-5 and D1B-W1 are on the Fremont Ranch close to Kesterson Ponds 1 and 2, and well KR-307B is approximately 1.3 km east of well KR-17 (see Fig. 1). Water levels in these wells exhibit a seasonal variation; the water level falls from its shallowest depth in February-March to its deepest level in late September and early October. In addition to the seasonal variation there also appears to be a trend of increasing water table depth over the two-year observation period in the wells closest to Kesterson Reservoir. The water table drop is concentrated at the junction of Ponds 1 and 2 (Well D1B-W1), where a 1.5 m drop was observed at the time of the 1988 EM survey. As one moves radially away from this location, the change between the two years decreases until far away from the ponds (Well KR-307B) the drop is only 0.04 m. Consequently, the drop in water level is attributed primarily to the drying out of Kesterson Reservoir.

The inverse modeling results, described in the preceding section, support a falling groundwater level to some extent. Most of the 1987 inversions of the lines close to the ponds give a first layer thickness of between 1.0 and 2.0 m. The results of the 1988 data set, while much more variable, seem to indicate a thickness 2.0 to 3.5 m.

Since saturation is a key parameter in bulk rock conductivity, a drop in the water table has an important influence on the electromagnetic instrument readings. To quantify this effect, varying water table depths and first-layer saturations were imposed on the four-layer approximation of the local hydrogeology (Fig. 20b). The depth to the water table ranged from 1.0 to 3.0 m in 0.5 m steps, and the first-layer saturation ranged from 50 to 80% in 10% steps. The results are shown in Figure 22. Decreasing the saturation results in a significant decrease in each of the instrument readings. A drop in the water table also lowers instrument readings, but to a lesser extent.

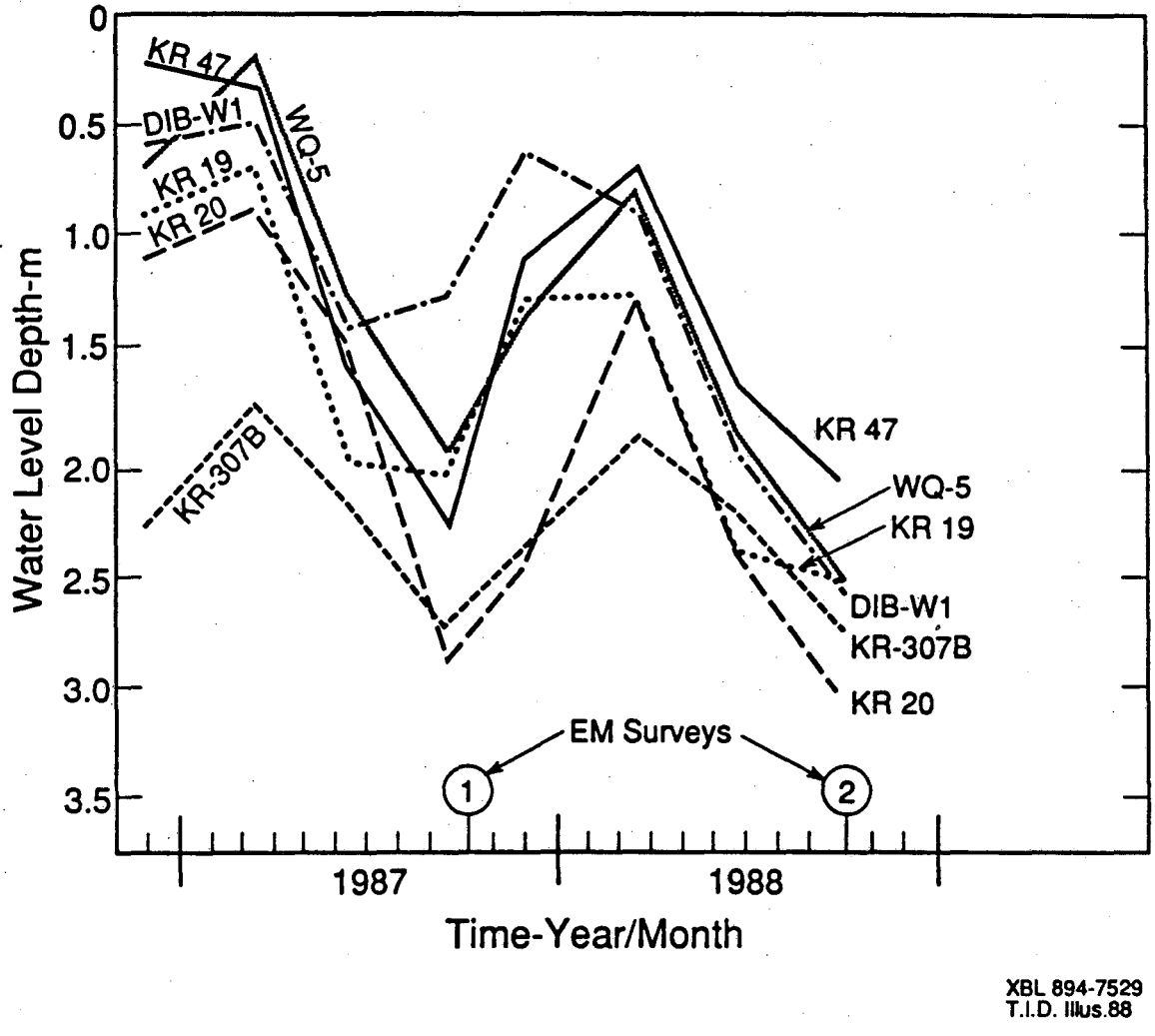

Figure 21. Water level depth changes in U.S. Bureau of Reclamation observation wells near Ponds 1 and 2 of the Kesterson Reservoir. Well locations are shown in Figure 1. Ground conductivity measurements were conducted at times 1 and 2.

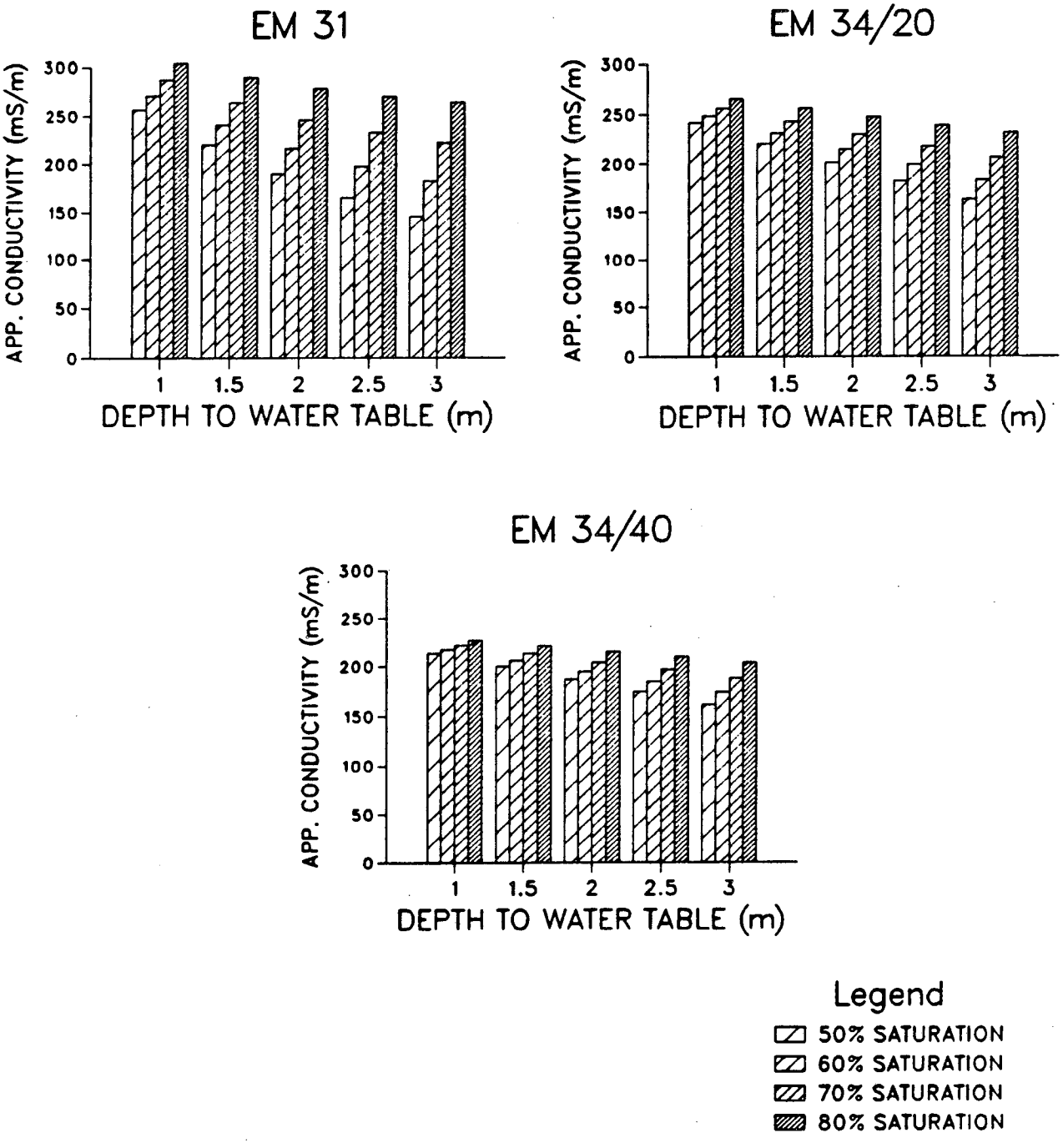

Figure 22. Effect of variable water table depth and first-layer saturation on the apparent conductivity measured by each instrument. The four-layer model of the hydrogeology was used for these calculations.

A combination of first layer desaturation from 80 to 60% and a water table drop from 1.5 to 2.5 m below the ground surface provides a reasonable explanation for the changes observed between the 1987 and 1988 averages (Fig. 18). For example, the combination of these two factors decreases in the apparent conductivities of each instrument: 92 mS/m for the EM31, 57 mS/m for the EM34/20, and 15 mS/m for the EM34/40. In comparison, the observed decreases average about 100, 40 and 10 mS/m, respectively (see Fig. 18).

Well data indicate that the water table decrease is centered at the junction between Ponds 1 and 2 (Figs. 1 and 21). Inspection of the pixel plots (Figs. 12-14) shows that the largest differences in the EM31 and EM34/20 between 1987 and 1988 are also located at this junction. This lends further credibility to the proposition that the observed decreases in near surface conductivities are due to decreases in both saturation and water-table depth.

Rainfall Effects

Measurable amounts of rain (0.01") were recorded at the Kesterson Reservoir rain gauge on the nights of October 11 and 13, 1988. If these same amounts fell at the nearby Fremont Ranch, infiltration would have formed a saturated surface layer approximately two to six mm thick (T. Tokunaga, 1989, personal communication). The pore water of this thin, saturated layer would contain salts dissolved from the soil, leading to a dramatic increase in its electrical conductivity. Since the electromagnetic instruments are very sensitive to the near-surface conductivity, the measurements taken after these rainfall events may have been significantly affected.

To investigate this possibility, data from Lines A–A′ and B–B′ (Fig. 4), recorded after the rain, were compared to the measurements at corresponding locations along Lines 1 through 7, recorded before the rain (Figure 23). The EM31 curves show a somewhat erratic agreement, with corresponding conductivity values differing from -27.1% to +115.3%. The pre- and post-rainfall curves agree more closely for the EM34/20 and EM34/40, but still exhibit significant discrepancies. Due to the large variability in the instrument readings, it was

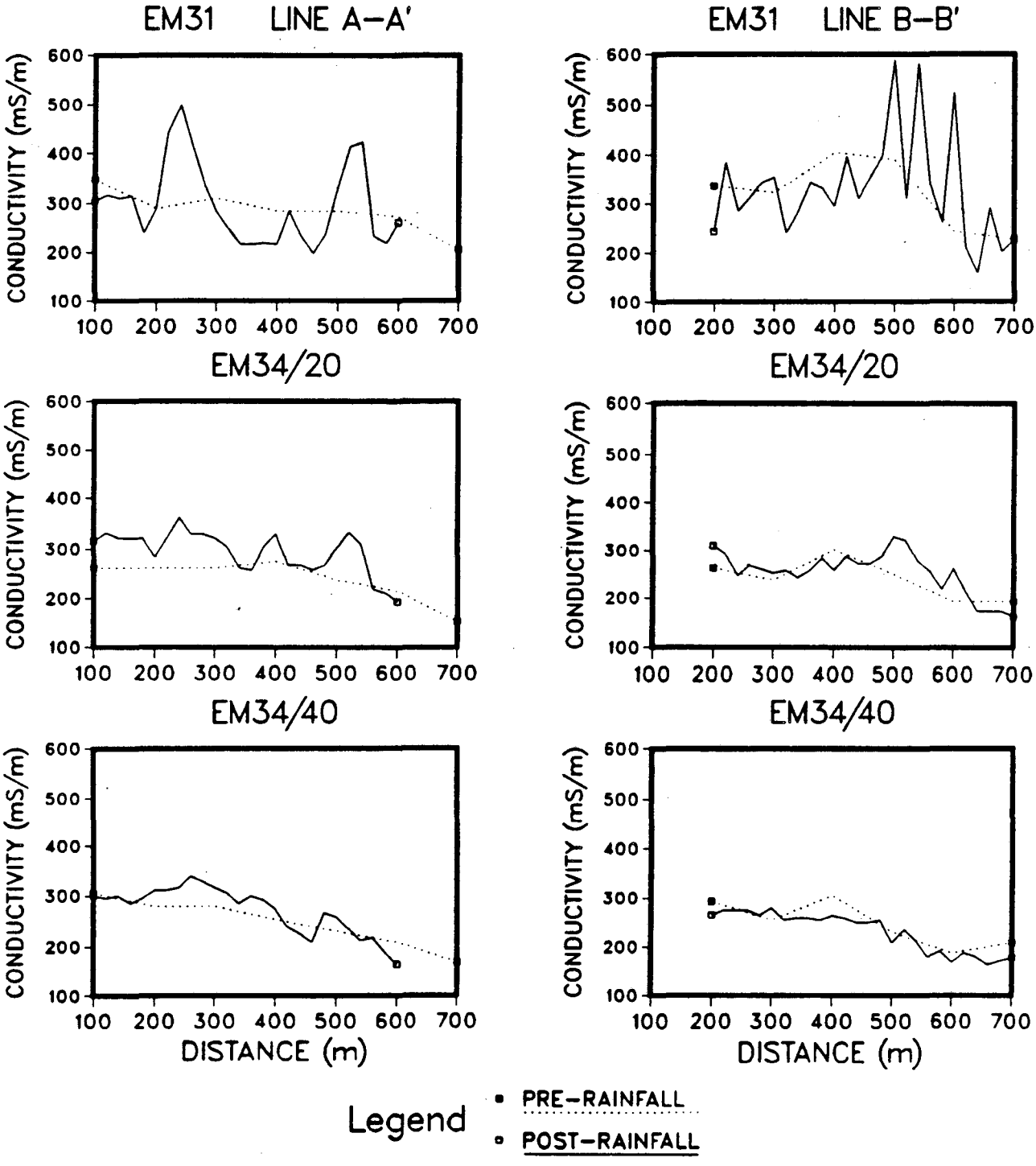

Figure 23. Comparisons of the apparent conductivities along Lines A–A′ and B–B′ (Fig. 4), recorded after a slight rainfall, to corresponding stations along Lines 1 through 7, recorded before the rainfall.

difficult to draw conclusions on rainfall effects from the field data alone.

Numerical modeling was then utilized to study the possible effects of small rainfall events on the data. Three generic cases were considered: a homogeneous half-space, and the two layered-earth models described above. To each case a thin surface layer was introduced with a conductivity 5 to 20 times greater than the pre-rainfall background value. For the calculations the thickness of the highly conductive surface layer was set equal to one and ten mm. The results were then compared to the same model without the surface layer. The models and calculated instrument readings are presented in Figure 24. By comparing the different cases, it is clear that the instruments are much more sensitive to the model used than to the effect of rain. In each case a 1 mm-thick surface conductor produces no change in the calculated readings. The addition of a 10 mm layer has the greatest effect on the EM31 readings, increasing them by up to 3.8%, while the EM34/20 and EM34/40 readings only change by an average of 1.0% and 0.5%, respectively. In comparison to the other sources of variability, such as lateral variability in near-surface conductivity and/or instrument accuracy, these changes are small. For instance, the highly variable saline conditions of the near-surface soil create variability on the order of 10-25% (see Fig. 5). Also, the instruments could be read to ± 0.05 scale division accuracy, which corresponds to approximately ±2% reading error. As these noise limits are greater than or equivalent to the maximum calculated changes predicted for a rainfall event, we conclude that the measurements made immediately following the two small rainfall events were not biased by the presence of a thin surface conductor.

Height of the EM31 Instrument

As the EM31 instrument is carried by a shoulder strap, changes in the heights of the various operators resulted in different instrument heights. To see how this affected the meter readings, numerical tests were run using instrument heights from 0.7 to 1.3 m in 0.1 m steps. To include the possible effect of saturation, cases were considered for first-layer saturations of 40, 50, and 60%. The four-layer approximation of the hydrogeology was used (Fig. 20b). The results (Fig. 25) show that each 0.1 m step in instrument height produced a change of

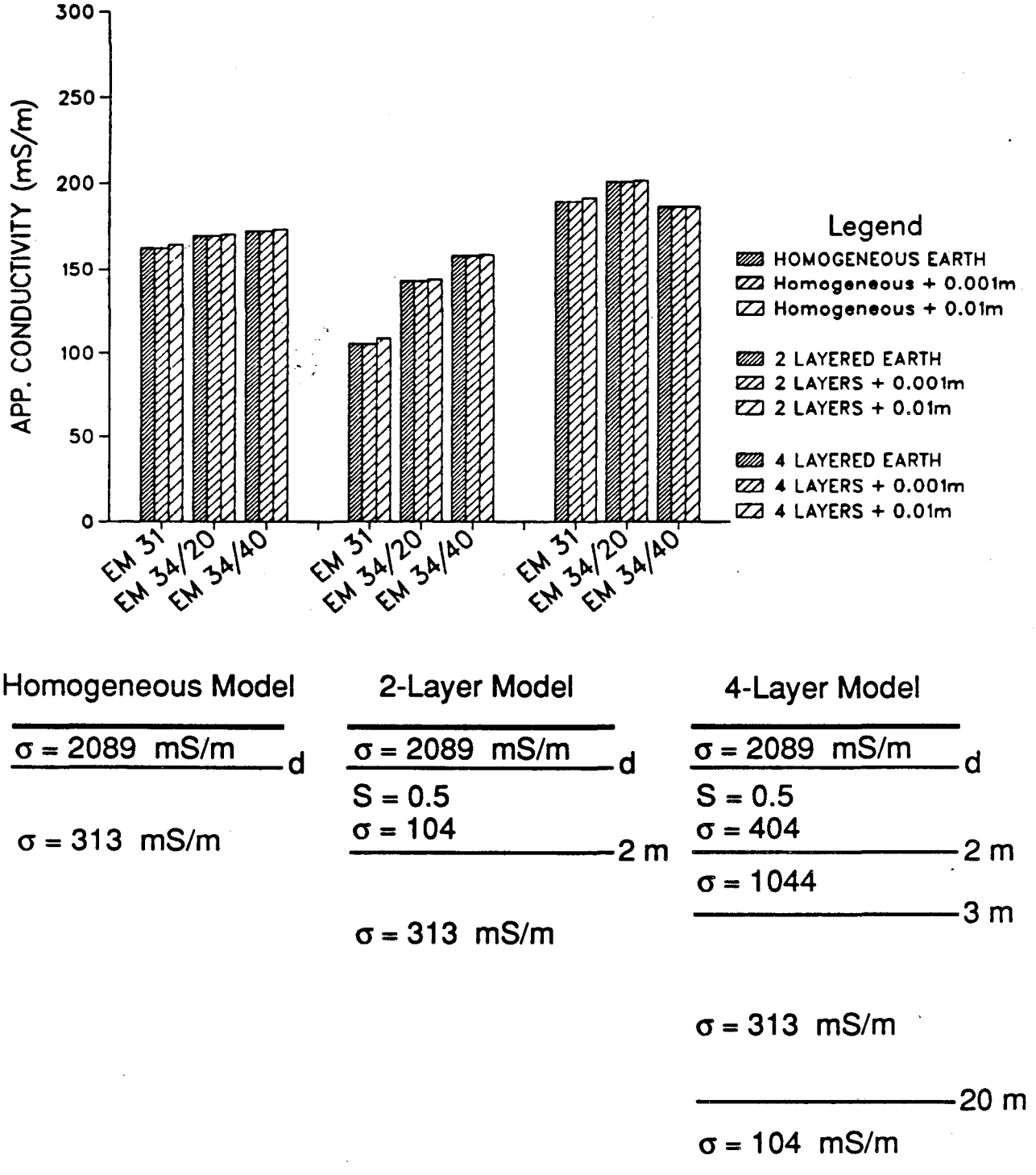

Figure 24. Models and results of a calculated pre- and post-rainfall event. Numbers given are the bulk rock conductivities; "d" equals the thickness of the rain-water saturated surface layer, 0.001 and 0.01 m. Note that the models are not drawn to scale.

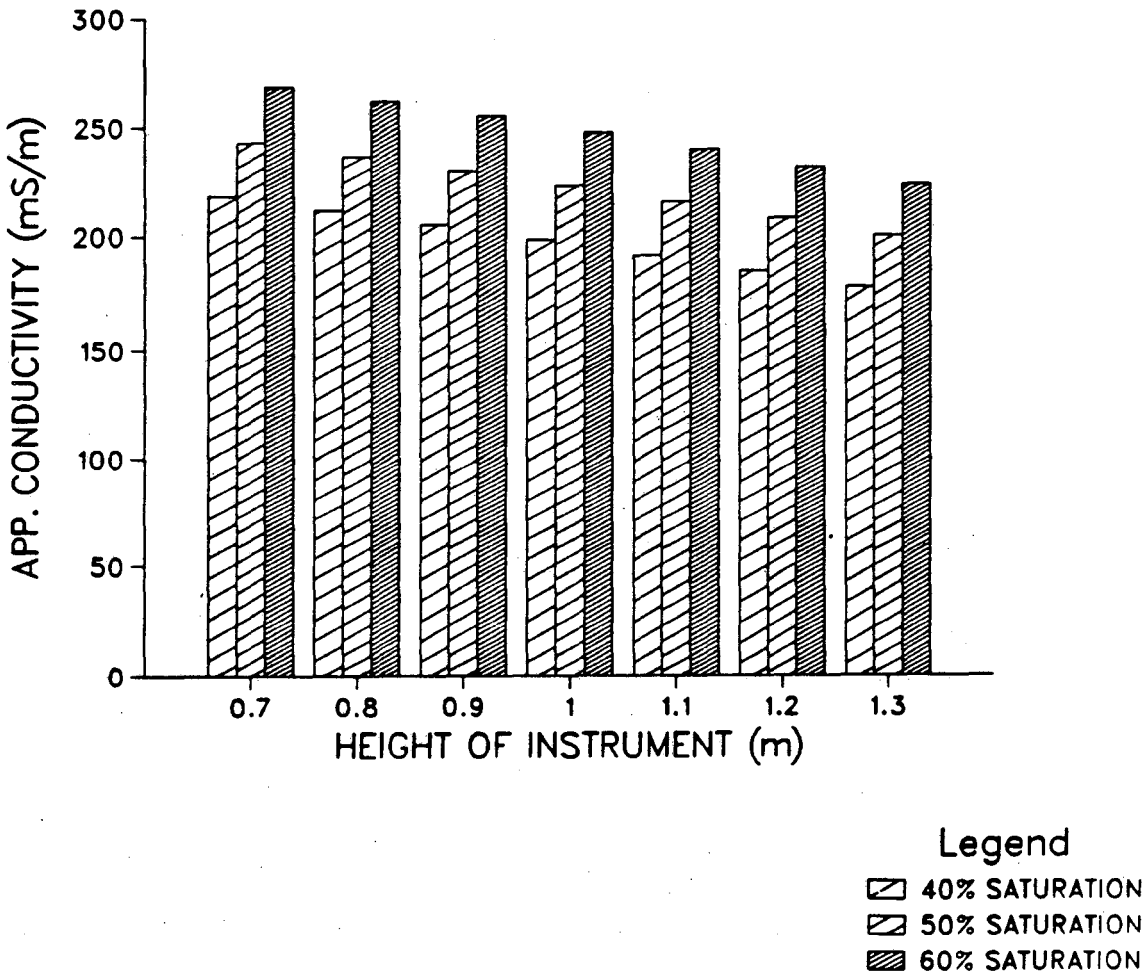

Figure 25. Calculated response of the EM31 instrument to a change in the height above the ground surface at which the measurement was made. The four-layered model of hydrogeology (Fig. 20b) was used for these calculations.

approximately 7 mS/m in the instrument reading, corresponding to a change no greater than 3%. This varied only slightly with changes in saturation.

Three taller than average operators surveyed Lines 6 and 7 in 1987 and Lines 0, 1, 2, 5, 6 and 7 in 1988. The taller surveyors carried the instrument approximately 0.2 m higher than the others, resulting in readings which were consistently 15 mS/m less than on other lines. This difference is small in relation of the magnitude of the readings, but may explain some of the differences of the EM31 averages between 1987 and 1988.

Non-Uniform Conductivity of the Surface Layer

The surface layer may have a gradational conductivity due to vertical variations in the distribution of clays and soluble salts. To determine what effect this would have on the instrument readings, the first layer was subdivided into seven thin layers. The conductivity of the pore water within each of the sub-layers was changed in non-uniform increasing or decreasing steps. The models and results are presented in Figure 26. Only the EM31 readings are significantly altered, but as the greatest change was only 2.4%, we conclude that instrument readings are insensitive to the vertical heterogeneity of the first layer.

Conclusions

Ground conductivity surveys done in October 1987 and repeated in October 1988 over part of the Fremont Ranch adjacent to Kesterson Ponds 1, 2 and 5 reveal a highly saline near-surface environment. Apparent conductivities for both years exceed 150 mS/m everywhere in the survey area for all three depths of investigation. Similar EM31 background levels were reported by Hanson and Grismer (1987) for the Mendota area, approximately 30 miles south of Kesterson, indicating that saline conditions as observed on the Fremont Ranch are typical for the soils on the west side of the San Joaquin Valley.

The primary objective of the survey was to locate and monitor the migration of a saline plume of agricultural drainwater from the San Luis Canal which was used to fill the ponds between 1981 and 1986. In both years conductive anomalies were found adjacent to Ponds 1,

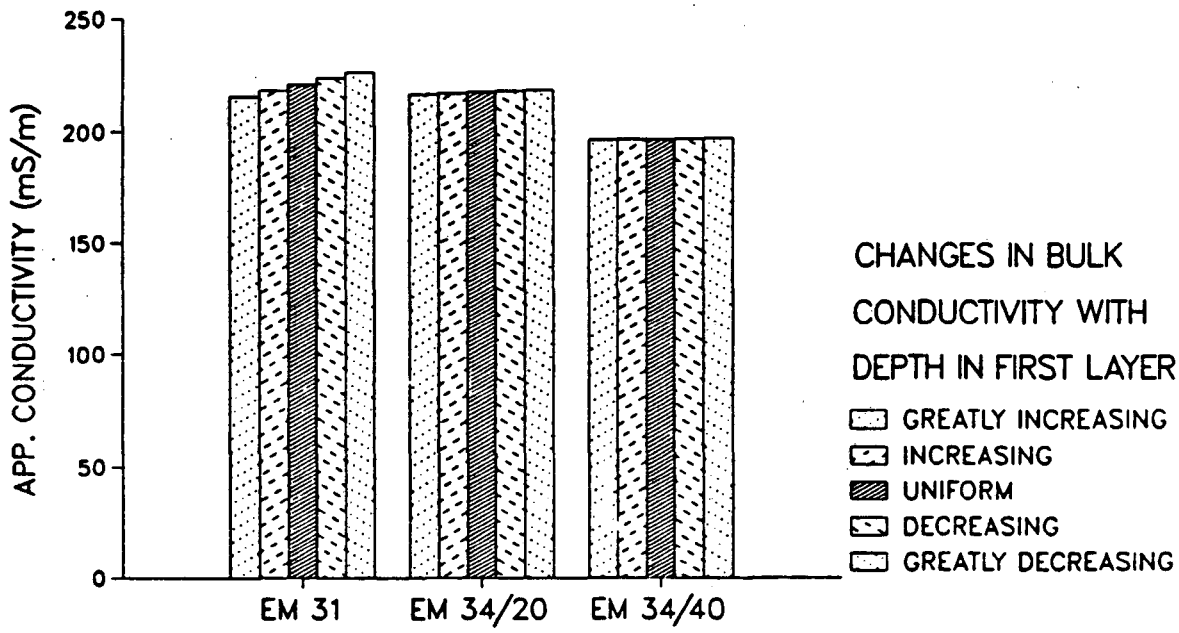

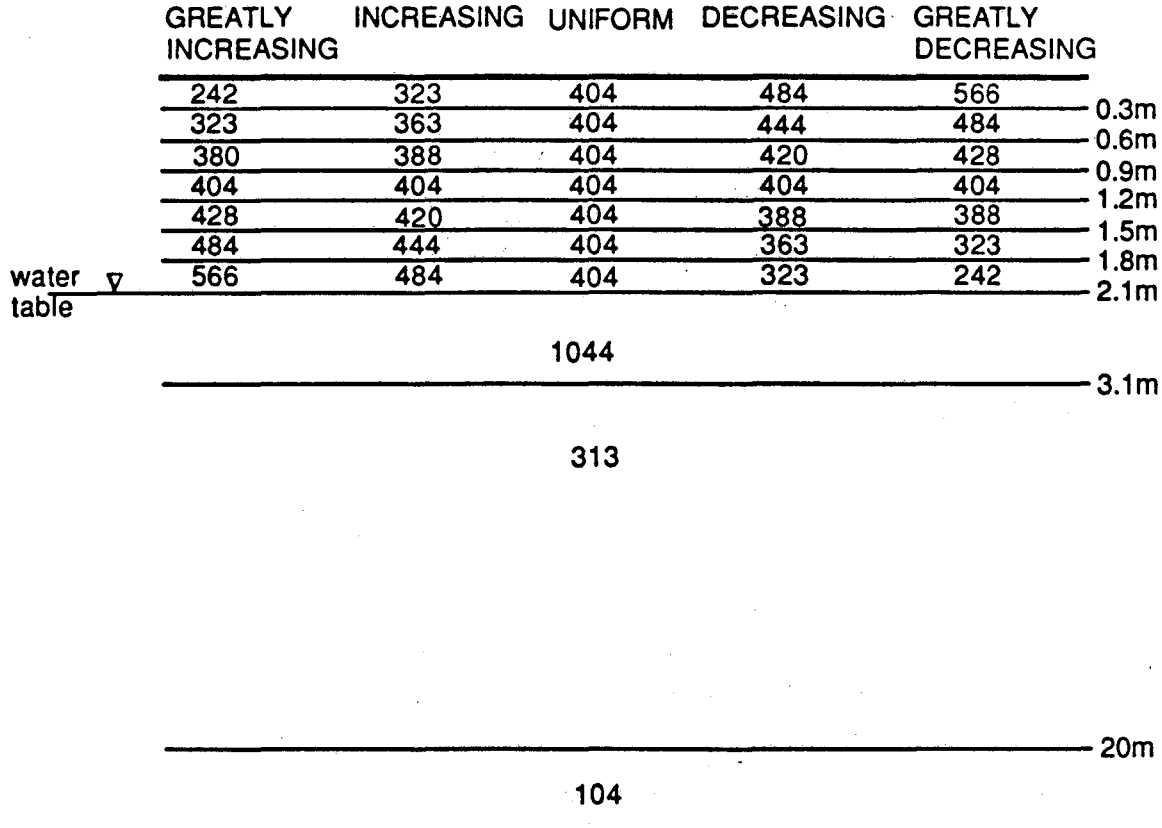

Figure 26. The effect of variable bulk conductivities (mS/m) in the unsaturated zone, due to a gradational distribution of salts, on observed instrument readings. Note that the models are not drawn to scale.

2 and 5. On the basis of their location, shape, and magnitude, the anomalies appear to be caused by infiltration and migration of the plume. The maximum lateral extent of migration is approximately 300 m adjacent to Pond 2, the principal inlet point for the agricultural drain waters. Less migration has occurred adjacent to Ponds 1 and 5; about 200 m at Pond 1 and less than 100 m adjacent to Pond 5.

A large decrease is seen in the surface conductivity between the 1987 and 1988 surveys. Water level data from several wells in the area and numerical modeling indicate that the lower apparent conductivities are primarily due to lower water table and drier near-surface conditions. Cessation of flooding Kesterson Reservoir is believed to be the primary cause for the drier conditions.

Inverse modeling and a limited statistical analysis of the data support these findings. For the numerical inversions of Line X–X′, a line running nearly perpendicular to Pond 2, the conductivity of the aquifer decreases to background values at a distance of about 300 m from the pond. The first layer conductivities and thicknesses decrease in 1988 suggesting a less conductive surface environment. Statistical analysis of the mean values along each survey line show significantly higher values adjacent to the ponds with levels returning to near background values about 300 m from the property line. Once again a significant decrease is seen in the near-surface conductivities in 1988.

Comparison of the 1987 and 1988 results suggest that the plume of saline drainwater has, to some degree, mixed with the better quality water used to flood the ponds in 1986-87. However, no significant migration of the leading edge of the plume was seen between the two years. This was probably due to the large spacing of the EM survey lines (100 m), which was not adequate to detect migration at an estimated rate of 5 to 50 m/year.

Discrete anomalies, with higher than average conductivities, exist away from the ponds. Their widespread nature suggests they are unrelated to the operation of Kesterson Reservoir. In fact, several of these correlate with natural drainage features, such as a slough and an oxbow lake. Other discrete anomalies correlate with areas that remain bleached throughout the

wet months, indicating very saline soil conditions.

Acknowledgments

The authors would like to thank the Freitas family for allowing LBL onto their ranch to make the measurements. We would like to thank, in particular, the many at LBL who helped with the field work in 1987 and 1988. These include Ray Solbau, Don Lippert, Alex Becker, David Alumbaugh, Cliff Schenkel, Joel Ita, Kurt Nihei, Cindy Yates and Qiang Zhou. The authors would like to extend special gratitude to Diana Parks and Leslie Boyd for their help in compiling this paper. The pixel plot program was written by John Peterson.

This work was supported by the U.S. Bureau of Reclamation under Agreement No. 7-AA-20-04710. The Lawrence Berkeley Laboratory is operated for the U.S. Department of Energy under Contract No. DE-AC03-76SF00098.

References

Anderson, W. L., 1979, Computer Program. Numerical integration of related Hankel transforms of order 0 and 1 by adaptive digital filtering: *Geophysics*, 44, 1287-1305.

Archie, G. E., 1942, The electrical resistivity log as an aid in determining reservoir characteristics: Trans. A.I.M.E., 146, 54-67.

Benson, S. M., 1988, Characterization of the hydrologic and transport properties of the shallow aquifer under Kesterson Reservoir, Merced County, California: Ph.D Thesis, University of California, Berkeley, CA.

Bussain, A. E., 1983, Electrical conductance in a porous medium; *Geophysics*, 48, 1258-1268.

Clavier, C., Coates, G. and Dumanoir, J., 1984, Dual water model for the interpretation of shaley sands: *Soc. Petr. Eng. J.*, April, 153-168.

Earth Sciences Division, 1986, Hydrological, geochemical, and ecological characterization of Kesterson reservoir: Second Progress Report (Dec. 1985 - June 1986): Lawrence Berkeley Laboratory, LBID-1188, 88 p.

Earth Sciences Division, 1987, Hydrological, geochemical, and ecological characterization of Kesterson Reservoir: Annual Report, Lawrence Berkeley Laboratory, LBL-24250.

Earth Sciences Division, 1989, Hydrological, geochemical and ecological characterization of Kesterson reservoir: Ninth Progress Report (Oct 1988 - Dec. 1988), Lawrence Berkeley Laboratory, LBID-1483, 35 p.

Fitterman, D. V., Meekes, J. A. C. and Ritsema, I. L., 1988, Equivalence behavior of three electrical sounding methods as applied to hydrogeological problems: presented at the 50th Ann. Mtg. and Tech. Exhib. Europ. Assoc. Expl. Geophys., The Hague, The Netherlands, 6-10 June, 1988.

Flexser, S., 1988, Lithologic composition and variability of the sediments underlying Kesterson Reservoir as interpreted from shallow cores: Lawrence Berkeley Laboratory, LBL-25586, 38 p.

Goldstein, N. E., Alumbaugh, D. and Benson, S. M., 1988, Ground conductivity measurements adjacent to the Kesterson Pond 1, 2, and 5: Lawrence Berkeley Laboratory, Technical Report LBL-24657, 25 p.

Hanson, B. R., and Grismer, M. E., 1987, A geophysical approach to evaporation pond siting and drainage design survey: 1986-1987 Technical Progress Report, U.C. Salinity/Drainage Task Force, Division of Agriculture and Natural Resources, Univ. of California, Davis.

Keller, G. V. and Frischknecht, F. C., 1966, Electrical methods in geophysical prospecting: Pergamon Press, New York, 517 p.

McNeill, J. D., 1980, Electromagnetic terrain conductivity measurements at low induction numbers: Geonics Limited, Mississagua, Ontario, Technical Note TN-6.

McNeill, J. D., 1985, EM34-3 measurements at two intercoil spacings to reduce sensitivity to near-surface material: Geonics Limited, Mississagua, Ontario, Technical Note TN-19.

McNeill, J. D., 1986, Rapid, accurate mapping of soil salinity using electromagnetic ground conductivity meters: Geonics Limited, Mississagua, Ontario, Technical Note TN-18.

Mendenhall, W., 1975, Introduction to probability and statistics: *Duxbury Press*, North Seltuate, MA, p. 400-401.

Waxman, M. H. and Smits, L. J. M., 1968, Electrical properties in oil-bearing shaley sands: *Soc. Petr. Eng. J.*, Trans. Am. Inst. Min. Metall. Petr. Eng., 243, 107-122.

Appendix A

Principles of Electromagnetic Measurements

The electromagnetic measurement of ground conductivity relies on the laws of the electromagnetic induction. Although the mathematical formulation is rather complicated, the basic principles, as diagramed in Figure A-l, are simple. A transmitter coil (T) energized with an alternating current produces a time-varying magnetic field (H_p) that induces weak eddy currents in the earth. Because the ground is conductive these eddy currents decay with depth, limiting the depth of investigation. However, the eddy currents produce a secondary magnetic field (H_s) that is detected along the primary field (H_p) by a receiver coil located a known distance away from the transmitter. The strength of the secondary field is a function of ground conductivity, frequency of the current, and transmitter-receiver separation (McNeill, 1980). If the operating frequency and separation are known, the apparent ground conductivity can be determined. In practice, it is possible to obtain readings of the weak secondary field in the presence of the much stronger primary field by designing the receiver to measure the quadrature component of the EM field; i.e., that part which is 90° out-of-phase with the primary field.

Causes of Ground Conductivity Anomalies

Laboratory studies show that the electrical conductivities of many types of rocks can be expressed through an empirical expression known as Archie's law (Archie, 1942) which states that rock conductivity is a function of ionic conductivity of the pore fluid and geometry of the flow paths; viz.,

$$\sigma_B = a\, \sigma_w\, (\phi^m\, S^2), \qquad \text{(A.1)}$$

where

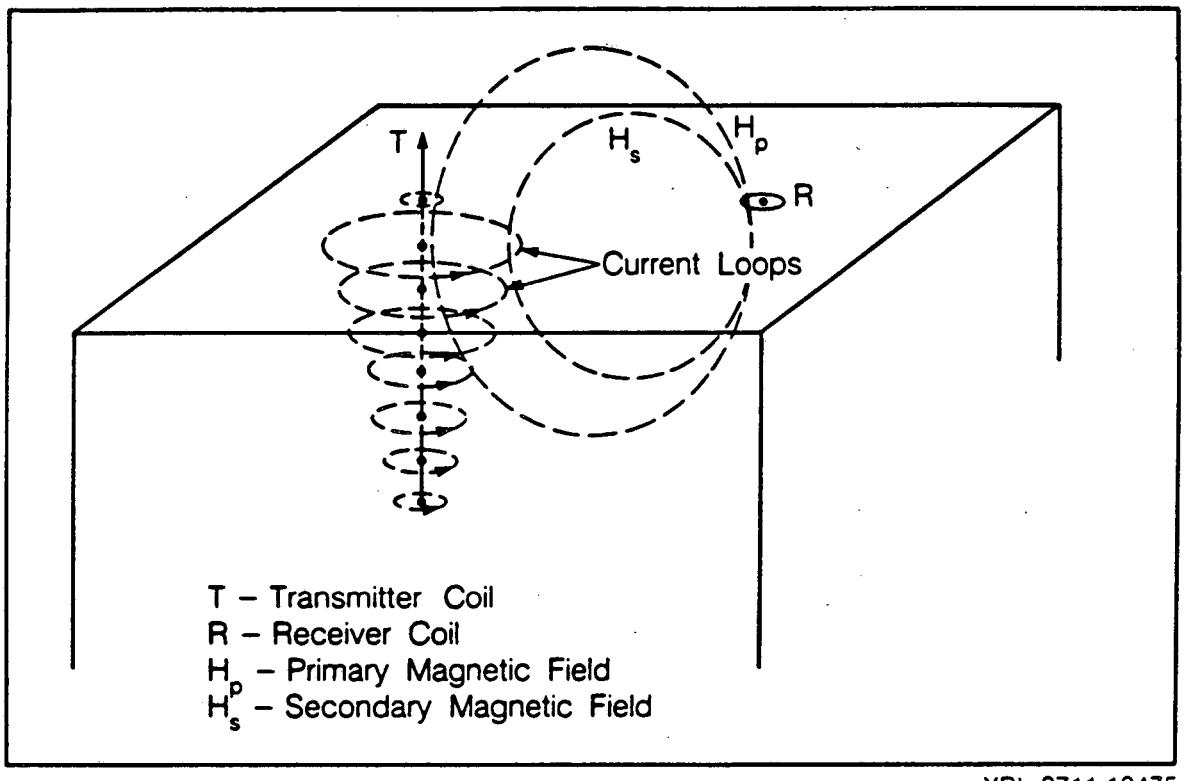

XBL 8711-10475

Figure A1. Simplified diagram illustrating the principles of electromagnetic induction and ground conductivity measurements. A primary EM field H_p is generated by horizontal loop transmitter T. Horizontal loop receiver R, a known distance away, detects both H_p and a secondary EM field H_s whose strength depends on the ground conductivity beneath the loops.

σ_B = the bulk conductivity of the rock,

σ_w = pore fluid conductivity,

ϕ = average connected porosity,

S = water saturation (S > 0.5),

a,m = coefficients, determined experimentally, that depend on rock type and fracture porosity (or cementation of the rock).

For most soils and rocks the bulk conductivity is strongly dependent on pore-water conductivity, σ_w, which is mainly a function of water salinity and temperature. Temperature increases water conductivity by making water a better solvent and reducing its viscosity. In rocks where conductive minerals also contribute to the bulk conductivity, Eq. A.1 may be replaced by one of several alternative expressions which researchers have proposed to account for the dual conduction mechanisms.

For conditions typical of unconsolidated sandy rocks saturated with saline drainwater, such as found at Kesterson (ESD, 1987), the parameters are approximately

$a = 0.88$

$m = 1.37$

$\phi = 0.35$

$S = 1.0$

$\sigma_w = 1{,}300$ mS/m

where ϕ is based on analysis of Kesterson soils and σ_w is a reasonable estimate of the conductivity of the agricultural drainwater. Inserting these values into Eq. A.1 gives a bulk rock conductivity of 270 mS/m. The calculated bulk rock conductivity will be dependent on the value chosen for a and m, but the bulk rock conductivity will invariably be much less than the con-

ductivity of the pore fluid. It should be noted that the calculated value of 270 mS/m is very close to the values obtained by means of inversion for the saturated second layer along Line X–X′ (Fig. 17).

Under natural conditions, σ_B can vary substantially both laterally and vertically, depending on depositional and post-depositional processes that affect porosity, depth to water table, and pore water salinity. Variations in σ_B may show up sharply in electric well logs but are greatly smoothed out by the volume averaging that occurs in measurements with the EM31 and EM34-3. At the risk of oversimplification, most of the averaging may be visualized as occurring with a semi-hemispheric volume whose radius is approximately equal to the depth of exploration for the particular instrument. Approximate depths of exploration for the EM31 and EM34 are listed in Table 1 for typical earth conditions. This depth is defined as the depth at which an electromagnetic plane wave decays to 1/e (or about 37%) of its amplitude at the surface. Because the attenuation of electromagnetic waves in the earth is proportional to $(\sigma_B)^{1/2}$, the actual depth of exploration for the instruments used in the Kesterson environment will be about one third those usually quoted for typical earth conditions (McNeill, 1986).

Table 1

Depth of Exploration of Geonics

Ground Conductivity Meters

(McNeill, 1986)

Instrument	Intercoil Spacing (m)	Transmitter Frequency (kHz)	Approximate Depths of Exploration (m)	
			Typical Conditions	Kesterson Conditions
EM31	3.7	9.8	7.0	2.2
EM34-3	20	1.6	15	4.8
EM34-3	40	0.4	30	9.6

Instrumentation

The EM31 consists of two coplanar loops mounted on a rigid boom, and is carried on a shoulder strap. In normal operation the EM31 is operated in a vertical dipole (VD) configuration, i.e., the coil planes are horizontal. With its intercoil spacing fixed at 3.7 m, the EM31 has the smallest depth of exploration of the three readings taken. The EM31 reading is sensitive to the height of the coils above the ground. Unless all measurements are made with the instrument lying on the ground, readings will vary with the height of the operator. Calculations presented earlier in this report indicate that variations of about 7 mS/m per 0.1 m difference in instrument height can occur when operators of different heights carry the instrument by the shoulder strap provided.

The EM34-3 uses two circular coils, each about a meter in diameter, connected by cable to the electronics. Intercoil separations of 10, 20 or 40 m are allowed and are switch selectable. We used coil separations of 20 and 40 m to achieve a greater depth of exploration than possible with the EM31. The EM34-3 requires a two-person crew, but we ran all surveys with at least one additional person to flag stations and record the meter readings.

The EM34-3 coils may be held in a horizontal-coplanar fashion to produce a vertical magnetic dipole (the VD configuration) or the coils can be set on the ground in a vertical-coplanar fashion to produce a horizontal magnetic dipole (the HD configuration). The VD configuration provides twice the exploration depth of the HD configuration, and is more sensitive to lateral conductivity variations, such as narrow conductive channels. However, the VD mode readings are highly sensitive to coil alignment, and can be highly inaccurate under the extremely high conductivity condition encountered in the Kesterson Reservoir area. For these reasons we did not use the EM34-3 in the VD mode.

Figure A-2 shows the relative sensitivity of the EM34 to ground conductivity over a homogeneous earth for the VD and HD coil configurations (McNeill, 1980). The curves are plotted against depth normalized by the intercoil separation. Most of the HD response arises from induced currents near the surface; only a small part of the meter reading is affected by

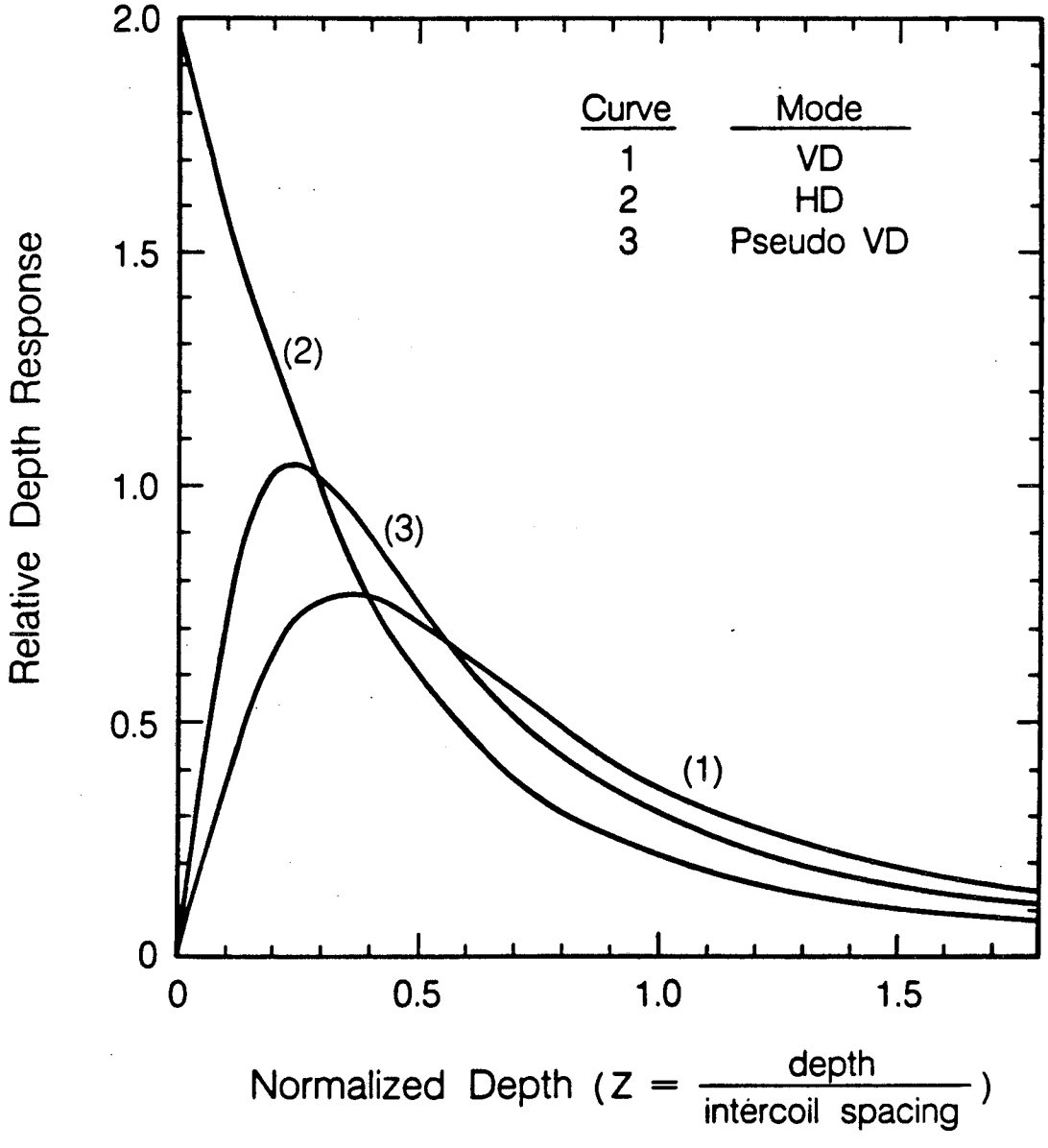

Figure A2. Relative induction response functions for the EM31 and EM34 instruments in the vertical dipole (VD) and horizontal dipole (HD) modes. Also shown is the response function for the pseudo-VD.

currents deeper than half the coil separation. On the other hand, the surficial conductivity contributes little to the meter reading in the VD mode. Due to coil alignment errors and the highly conductive nature of the ground within the survey area, the VD mode could not be used directly. It is possible, however, to transform HD data taken at two intercoil separations and obtain a set of data which is affected by the earth, in theory, as shown by response Curve 3 in Fig. A-2. Because of this similarity to the VD response curve, we refer to Curve 3 as a pseudo-VD response.

Inherent in the design of the EM31 and the EM34-3 is that the inductive response of the earth, given by dimensionless induction number B, is small:

$$B = \frac{\omega \mu_o \sigma s}{2} \ll 1, \tag{A.2}$$

where

σ = ground conductivity (S/m),

ω = the instrument operating frequency in radians = $2\pi f$

f = frequency (Hz),

μ_o = permeability of free space ($4\pi \times 10^{-7}$ H/m), and

s = intercoil spacing (m).

For this condition the conductivity is linearly proportional to the ratio of secondary to primary magnetic field. The resulting equation is

$$\sigma = \frac{4(H_s)}{\omega \mu_o s^2 (H_p)}, \tag{A.3}$$

where

H_s = quadrature component of the secondary magnetic field, and

H_p = primary magnetic field.

In areas of high ground conductivity (σ > 30 mS/m) such as found at the Fremont Ranch, Eq. A.3 no longer holds; the inductive coupling between transmitter and receiver coils becomes

non-linear and the meter readings must be corrected to give a true estimate of σ. To save time and reduce the chance of introducing errors, we generated a set of instrument responses for a wide range of homogeneous earth conductivities using program PCLOOP supplied to us by Geonics Ltd. The correction values were stored in a separate program, and the three files of field data were corrected in a batch operation.

Sources of Measurement Error

Instrumental factors that could create differences between the 1987 and 1988 measurements can be referred to under the categories of instrumental accuracy and reading precision effects.

Measurement accuracy specifications for both types of instruments are quoted as ±5% at 20 mS/m; i.e., any two calibrated units of the same type of instrument operated in the same fashion should give meter readings within 10% of each other over ground that is not too conductive. Measurement accuracy is expected to worsen under highly conductive conditions, such as found near the Kesterson Reservoir, but instrument accuracy figures are not reported for these more extreme conditions.

Part of normal instrument error is due to non-linear deflection of the needle in the analog meter. To minimize this source of error, all operators were instructed to manually set the conductivity range switch on the receiver so that the needle position is within the upper half of the meter range where behavior is least non-linear.

Another small part of EM34 instrument error occurs because of coil misalignment. In the HD mode of operation which we used, the measurement is relatively insensitive to small misorientations of the receiver coil relative to the transmitter coil. In this mode a small error of angle θ in coil alignment produces only a cosine θ error in the apparent conductivity. Thus, a 10° misalignment of the coils produces < 2% error in the reading. During the surveys, it became a common practice for the EM34 operators to vary coil alignment in order to assure themselves that any error was within their ability to read the meter.

Measurement precision, which is a function of errors in reading the meter needle against a graduated scale, is ±2% of full scale for both EM31 and EM34. As most readings were taken on the 300 mS/m full-scale range, the typical "parallax" errors are within ±6 mS/m.

Based on these three sources of error, our overall instrument accuracy is calculated to be ±6% of the full scale range, which corresponds to ±18 mS/m. Information on the performance of the EM31 under high to extremely high ground conductivity conditions has been deduced from a survey conducted along several long east-west transects, near Mendota, California, 30 miles south of the Kesterson Reservoir by Hanson and Grismer (1987). Their data, collected at 15-m spacings, gave ground conductivities mainly in the interval of 100 to 200 mS/m, somewhat below the range we obtained over the Fremont Ranch. The authors smoothed their data by means of a 7-point moving average and then calculated residual EM31 data curves by subtracting the smoothed from the unsmoothed data. The residual curves consist of a relatively uniform train of oscillations with zero mean. The envelopes of the oscillations for six transects, each 8.0 km in length, indicate noise levels within ± 10 mS/m at 150 mS/m (≈±7% at 150 mS/m) and within ± 30 mS/m at 250 mS/m (≈±12% at 250 mS/m). These figures represent a combination of instrument error, reading error and spatial variability with lateral dimensions of about 30 m or less. Similar variability was observed for the EM31 obtained as part of this survey, as indicated in Figures 5 and 23.

As we also discovered, instrument noise is exacerbated by weak transmitter batteries. Low primary field strength may not be immediately apparent from the meter readings during a survey. Although the readings may seem all right, Geonics engineers report that weak batteries will cause the meter readings to be either consistently higher or lower by an unpredictable amount (F. Snelgrove, 1989, personal commun.).

LAWRENCE BERKELEY LABORATORY
TECHNICAL INFORMATION DEPARTMENT
UNIVERSITY OF CALIFORNIA
BERKELEY, CALIFORNIA 94720